Luminescent polymer blends in hybrid organic-inorganic polymer light-emitting devices (HyPLEDs)

Hyun-Jung Lee

Advanced Materials Engineering Major

Mechanical and Advanced Materials Engineering

Graduate school of UNIST

2012

Luminescent polymer blends in hybrid organic-inorganic polymer light-emitting devices (HyPLEDs)

Hyun Jung Lee

Advanced Materials Engineering Major

Mechanical and Advanced Materials Engineering

Graduate school of UNIST

Luminescent polymer blends in hybrid organic-inorganic polymer light-emitting devices (HyPLEDs)

A thesis
submitted to the School of Mechanical and Advanced Materials Engineering
and the Graduate School of UNIST
in partial fulfillment of the
requirements for the degree of
Master of Science

Hyun-Jung Lee

12.05. 2011
Approved by

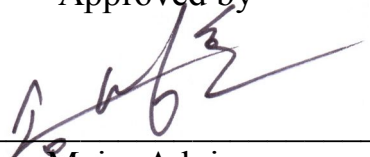

Major Advisor
Myoung Hoon Song

Luminescent polymer blends in hybrid organic-inorganic polymer light-emitting devices (HyPLEDs)

Hyun-Jung Lee

This certifies that the thesis of Hyun-Jung Lee is approved.

12.05. 2011

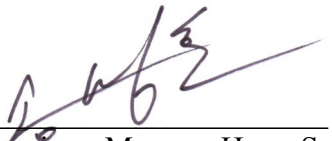

Thesis Supervisor: Myoung Hoon Song

Jeong Min Baik: Thesis Committee Member #1

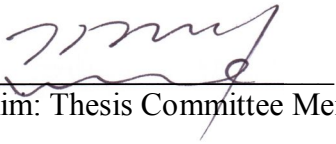

Jin Young Kim: Thesis Committee Member #2

Abstract

Organic/polymer based light-emitting diodes (OLEDs/PLEDs) have enormous technological significance for low-cost solution processing such as spin coating, dip coating and ink-jet printing. A recent promising approach toward air-stable devices without a low work function metal is to use inorganic metal oxides as charge injection and transport layer. In particular, solution processable n-type ZnO layer as electron injection/transport layer was mainly used in hybrid organic-inorganic polymer light-emitting diodes (HyPLEDs) and organic solar cells (OSCs). Based on HyPLEDs, PLED performance was optimized by blending luminescent polymers with various functional molecules or same fluorescent polymers. Blending approaches are generally considered to offer simpler device fabrication, higher device efficiency and performance. Here, we report a luminescent polymer blend system by mixing fluorescent polymer with ionic salt for hybrid organic-inorganic polymer light-emitting electrochemical cells (HyPLECs), and fluorescent red, green, and blue (RGB) polymers for white PLEDs (WPLEDs). Further development was achieved by attaching cholesteric liquid crystal (CLC) reflector in front of the surface of WPLEDs to obtain white circularly polarized (CP) electroluminescence (EL).

This thesis is organized as follow. An introduction of semiconducting polymers, characteristics of OLEDs and hybrid PLEDs with diverse transition metal oxide (TMO) layer are mainly described in the chapter 1. In particular, hybrid organic-inorganic polymer light emitting diode (HyPLEDs) are new type of top-emission device in which device can combine with n-type thin-film transistor (TFTs) for application to active matrix structure. The ZnO layer as a cathode material in the inverted configuration takes a role of the electron-injecting layer as they combine properties such as transparency, low resistance, and air-stability. In the chapter 2, we demonstrate enhanced device performance by using a blend of emissive polymer (“Super Yellow”) and mobile ionic liquid molecules (ILMs) in hybrid organic-inorganic polymeric light-emitting electrochemical cells (HyPLECs) with high air stability. The mobile anions and cations redistributed near each electrode/active layer interface make ohmic contacts, thereby enhancing current density and electroluminescence efficiency at relatively low operating voltage. Moreover, a luminescent blend of blue-emitting polymer (“M-blue”), orange-emitting dye (DCM), and ILMs was investigated to achieve white emission in HyPLECs. By using ILMs, we can observe the characteristics of LECs with low operating voltage and air stability of HyPLECs by introducing ZnO layer. Finally, we investigate RGB ternary blend in single active layer for white emission. WPLEDs using polymer blends showed low turn-on voltage, high brightness, efficiency, and color stability. Furthermore, we observed CP-EL by combination of WPLED and cholesteric liquid crystal (CLC) reflector.

Contents

List of Figures

Forward bias; carriers are injected through the triangular barrier at the anode (holes) and cathode (electrons) and meet within the polymer film where they radiatively recombine (electroluminescence).

Figure 1.11 Schematic representation of a single-layer organic light emitting diode. (a) A metal "band diagram" adjacent to HOMO/LUMO levels of an organic semiconductor is depicted. (b) Schematic functioning of a single layer OLED. (c) HOMO/LUMO levels and metal "band diagram" for electron injection.

Figure 1.12 OLED display revenue forecast.

Figure 1.13 (a) Passive and (b) active matrix OLED.

Figure 1.14 Device configuration of (a) conventional and (b) inverted structure.

Figure 1.15 (a) Device architecture of single F8BT layer HyPLEDs with SADMs on a ZnO surface (b) Chemical structures of carboxylic acid based SADMs: (i) negative dipole molecules (ii) positive dipole molecules. Schematic energy diagrams for flat band conditions of HyPLEDs with (a) unmodified ZnO, (b) negative, and (c) positive SADM modified ZnO. (d) Experimentally measured work functions of ZnO as a function of the _SADM using UPS.

Figure 1.16 Schematic energy-level diagrams at the n-type-metal-oxide/F8BT junction with and without the CPE having negative dipoles.

Figure 1.17 Illustration of spin-coating processing.

Figure 1.18 Schematic of the spray pyrolysis process.

Figure 1.19 The configuration for measuring PLED luminous intensity.

Figure 2.1 Device architecture of an LEC used in this study

Figure 2.2 Schematic representation of polymer LEC operation (a) before and (b) under an applied forward bias. (c) The recombination of injected electrons and holes in emissive layer caused by the redistribution of anions and cations.

Figure 2.3 The two models proposed for LECs operation with associated spatial distribution of the electric field shown underneath. (a) The electrochemical model. Injection of holes and electrons causes oxidation and reduction of the organic semiconductor close to the anode and cathode, respectively. Counter ions move to compensate the reduced and oxidized molecules, leading to the formation of p- and n-doped layers that extend into the bulk of the device. The high conductivities of the doped regions cause the electrode/organic interfaces to act as low-resistance contacts, allowing easy carrier injection. The radiative recombination of electrons and holes in the middle of the device depletes the charge carriers, leading to the formation of an undoped junction region across which the entire applied bias is dropped. (b) The electrodynamic model. Under an applied forward bias, a slight redistribution of the ionic charge occurs, leading to an excess of anions and cations at the anode and cathode, respectively. The accumulated ions cause a local enhancement in the electric field and — if the density of ions is sufficiently high — leave the bulk of the device virtually field-free. The electrons and holes diffuse through the field-free bulk and meet in the middle of the device where they recombine.

Figure 2.4 (a) Device configuration of HyPLECs using a blend of super yellow (SY) and ionic liquid molecules (ILMs). (b) Chemical structure of phenyl-substituted PPV copolymer, SY as a luminescent polymer and tetradecyltrihexylphosphonium bis(trifluoromethylsulfonyl)amide as mobile ILMs.

Figure 2.5 AFM images of SY:ILMs blend film with (a) 0, (b) 25, and (c) 35 weight % of ILMs.

Figure 2.6 Device characteristics of (a) current density vs. applied voltage (J-V), (b) luminance vs. applied voltage (L-V) and (c) luminous efficiency vs. current density (LE-J) curves with SY:ILMs blend films using different ILMs weight percent after initial forward bias of 5.0 V for 30 s for ion redistribution in polymer LECs with and without ZnO layers. (d) Electroluminescence spectra for pure SY and SY:ILMs (25%) blend film.

Figure 2.7 (a) Luminance versus voltage (L–V) characteristics for polymer LECs with and without the ZnO layer measured as a function of time in air atmosphere. (b) Comparison of the luminous efficiency (LE) at 50 cd/m^2 as a function of time for polymer LEDs with and without the ZnO layer.

Figure 2.8 (a) Current density-applied voltage-luminance (J-V-L) characteristics under forward and reverse bias of the HyPLECs fabricated with SY:ILMs _25%_ blend film. (b) Time response of current density (open symbol) and luminance (closed symbol) for FTO/ZnO/SY:ILMs (25%)/Au configuration under a forward bias of 3.2 V.

Figure 3.9 Normalized EL spectra of white emission in PLEDs with varying the composition of red polymer dopant.

Figure 3.10 CIE color diagram of white emission in PLEDs with varying the composition of red polymer dopant.

Figure 3.11 Color stability of white emission PLED with composition of M-blue:SY(0.075wt%):M-red (0.5wt%)

Figure 3.12 Color stability of PLED with composition of M-blue(99.4wt%):SY(0.075wt%):M-red (0.5wt%).

Figure 3.13 Current density (J) and luminance (L) versus applied voltage (V) for white emission device of ITO/PEDOT:PSS/M-blue(99.4wt%):SY(0.075wt%):M-red(0.5wt%)/LiF/Al configuration.

Figure 3.14 Luminous efficiency (LE) versus current density (J) for white emission device of ITO/PEDOT:PSS/M-blue(99.4wt%):SY(0.075wt%):M-red(0.5wt%)/LiF/Al configuration.

Figure 3.15 (a) The schematic device configuration for highly CP-EL from OLED and (b) corresponding structure of R-CLC reflector.

Figure 3.16 R- and L-CP-EL spectra from OLED devices with wide-PCLC films and transmittance spectra of wide-gap R-CLC reflective film.

Figure 3.17 Voltage-CP-EL plot of OLEDs with and without PCLC films. R and L polarizers were inserted to measure the R-CP-EL and L-CP-EL.

List of Tables

Chapter 1 Introduction

1.1 Objective and overview of the research

Organic light-emitting diodes (OLEDs)/polymer light-emitting diodes (PLEDs) are new generation technology suitable for applications such as lightweight flat panel or flexible displays and energy-saving solid state lighting. In recent decades, OLEDs have been the subject of significant research due to their cost-effective process.[1] In contrast to inorganic LED that crystals grown by expensive epitaxial methods such as molecular beam epitaxy or chemical vapor deposition, PLEDs can be fabricated with low cost solution processing such as spin coating, dip coating and ink jet printing methods. Moreover, the ability to chemically alter the materials in ways such as side-chain manipulation and copolymerization is excellent for device improvement and color tunability.

The first discovery of conductivity in organic materials was reported by using naphthalene and anthracene in the 1950s and early 1960s.[2-5] A breakthrough in conducting polymer synthesized was in 1977, when chemically doped polyacetylene was reported.[6] The conductivity of polyacetylene was 10^5 S/m with comparison of copper conductivity around 10^6 S/m. In the 1980s, the fabrication of electroluminescence cells using low molecular weight materials was reported from vacuum-sublimed molecular thin film devices.[7-14] Since Burroughes et al. found electroluminescence from conjugated polymer(CP) named poly(*p*-phenylenevinylene) (PPV) in 1990[1], the optoelectronic applications using CP such as OLEDs, organic solar cells, organic transistors, and so on have been shown in the past two decade.[13,15-20]

1.2 Theory of conductivity

1.2.1 Atomic and molecular orbitals of carbon materials

The most important characteristics of the conjugated polymers are their molecular structures with alternating single and double carbon-carbon bonds and the doping properties of the conjugated main chains. The alternating single and double bonds between adjacent carbon atoms of conjugated polymers render them semiconductor similar to more well-established inorganic semiconducting materials. However, the amorphous state of conjugated polymer is characterized by structure of weak electron screening and strong electron-lattice coupling. These chain defects and chain rotations require a variety of theories for describing the inherent optical and electrical properties. Conjugated polymers are formed from sp^2p_z hybridized carbon. There are two types of bonds in a conjugated polymer, which are σ-bonds correspond to the regions of overlapping orbitals between two nuclei and π-bonds form from the left overlapping p-orbitals in regions perpendicular to σ-bonds. The three in-plane σ-bonds create the "backbone". π-bonds are significantly weaker than σ-bonds as electron densities are more delocalized from the nucleus.

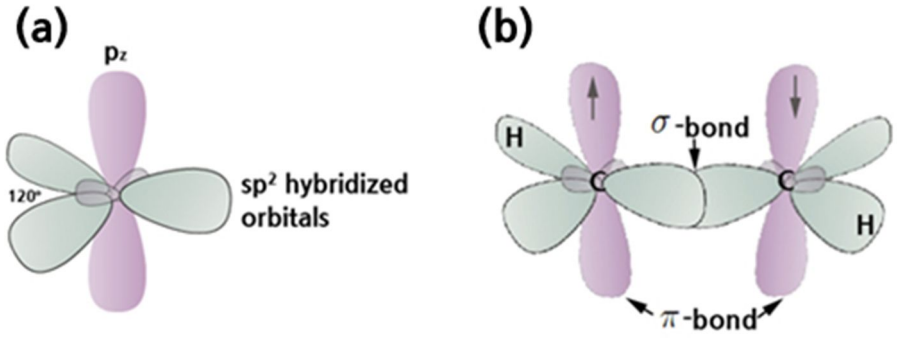

Figure 1.1 (a) A side view of sp2 hybridized atomic orbitals, (b) bonding in valence bond theory for conjugated polymers. The arrows represent electrons and their spin orientation.

Figure 1.1 shows sp^2p_z hybridized carbon and the resulting orientation of the leftover p_z orbitals. Single bonds along the backbone of the polymer are comprised of single sp^2 orbitals while the σ-bond of another sp^2 orbital in combination with the π-bond of the p_z orbital forms the double bonds. The remaining sp^2 orbital forms a σ-bond with hydrogen. There is a possibility of two same electrons to coexist at the same location and time, and this is prohibited from Pauli exclusion principle. Therefore, the two overlapped atomic orbitals split and form two new different energy (and shape)

orbitals called molecular orbitals. Molecular orbital (MO) theory approximates the molecular orbitals formed when two atoms come together as linear combinations of individual atomic orbitals. The quantum mechanical combinations result in bonding molecular orbitals that have lower energies and greater probabilities of the electrons residing between atoms and anti-bonding molecular orbitals that have higher energies with atoms unlikely to be between the molecules with energy values relating to the overlap between the two atomic orbitals. Figure 1.2 shows σ-/ π- bonding and the respective antibonding orbitals resulting from MO theory considerations for the 1s and 2p electron states. MO theory helps us better describe properties of conjugated polymers in expressions analogous to those of band theory for crystalline semiconductors because delocalized electrons inherent in the polymer structure account for its semiconductivity.

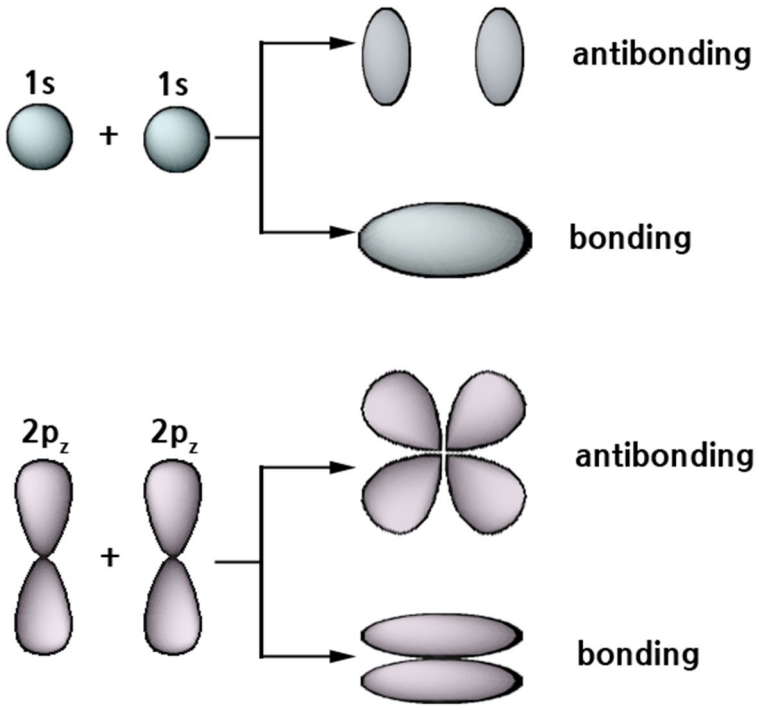

Figure 1.2 Bonding and anti-bonding orbitals in molecular orbital theory.

Figure 1.3 presents the MO theory-based picture of antibonding and bonding orbitals formed from the 2p orbitals of a single atom. As molecules become more complicated, the levels broaden into continuous bands. The highest occupied molecular orbital (HOMO) is the energy at the top of the band of occupied states while the lowest unoccupied molecular orbital (LUMO) is the first energy level in the unoccupied band. The HOMO is analogous to the top of the valence band (VB) and the LUMO, to the bottom of the conduction band (CB) in crystalline semiconductor physics; The gap

between the band gaps is typically the energy difference between the π and π^* energy levels. The band gap of these materials is within the semiconductor range of 1 - ~4eV, which covers the whole range from infrared to ultraviolet region.

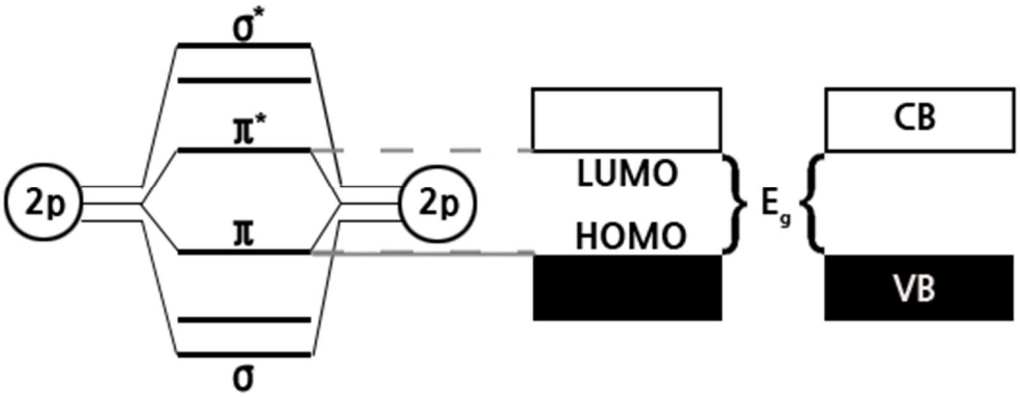

Figure 1.3 Molecular orbital theory schematic for 2p-states in a diatomic molecule and subsequent band formation.

1.2.2 Conduction mechanism – Soliton, polarton and bipolaron[21,22]

It is difficult to describe charge transport in conjugated polymer due to the absence of an ideal 3D periodic lattice in terms of inorganic semiconductor models.[23] Inorganic semiconductor materials have a 3D architecture characterized by infinite repetition of unit cell. Its structure can be described in terms of a lattice characterized by long-range order and strongly coupled atoms. This strong coupling results in the formation of long-range delocalized energy bands separated by a forbidden energy gap. Carriers within the semiconductor move along these energy bands with relatively large mean free path. Carrier scattering significantly affects the carrier mobility, which depends on the conductivity, effective mass of electrons, and the temperature. In conjugated polymer, the atoms are held together by weak van der Waals or London forces. The band structure appeared in the inorganic material can be easily disrupted due to this weak coupling and disorder in the system. Although organic molecular crystals still exhibit band conduction, excitations and interactions localized on individual molecules play a predominant role. It is important to consider both electron-lattice and electron-electron interactions to have insight into luminescence polymer and stability of polarons and bipolarons in modeling the optical and electrical properties of conjugated polymers. The Su-Schrieffer-Heeger (SSH) theory describes the electronic structure of conjugated polymers,[24] taking account of electron-phonon coupling. Another model that explains the electronic structure is the Peierls-Hubbard model, which also takes account of electron-electron coulombic interaction.[25,26] The model calculations give rise to a whole spectrum of "quasi-particles", both charged (net on-chain charge, e.g., by doping or charge injection) and uncharged. In general, n-type doping refers to a minority donor type dopant trapping a hole (or positive polaron) from the majority phase via donating an electron (or create a negative polaron) into the LUMO band of the majority phase, and p-type doping generally refers to a minority acceptor type dopant trapping an electron from the majority phase leaving a mobile hole (or positive polaron) at the HOMO band of the majority phase. These are shown in Figure 1.4.

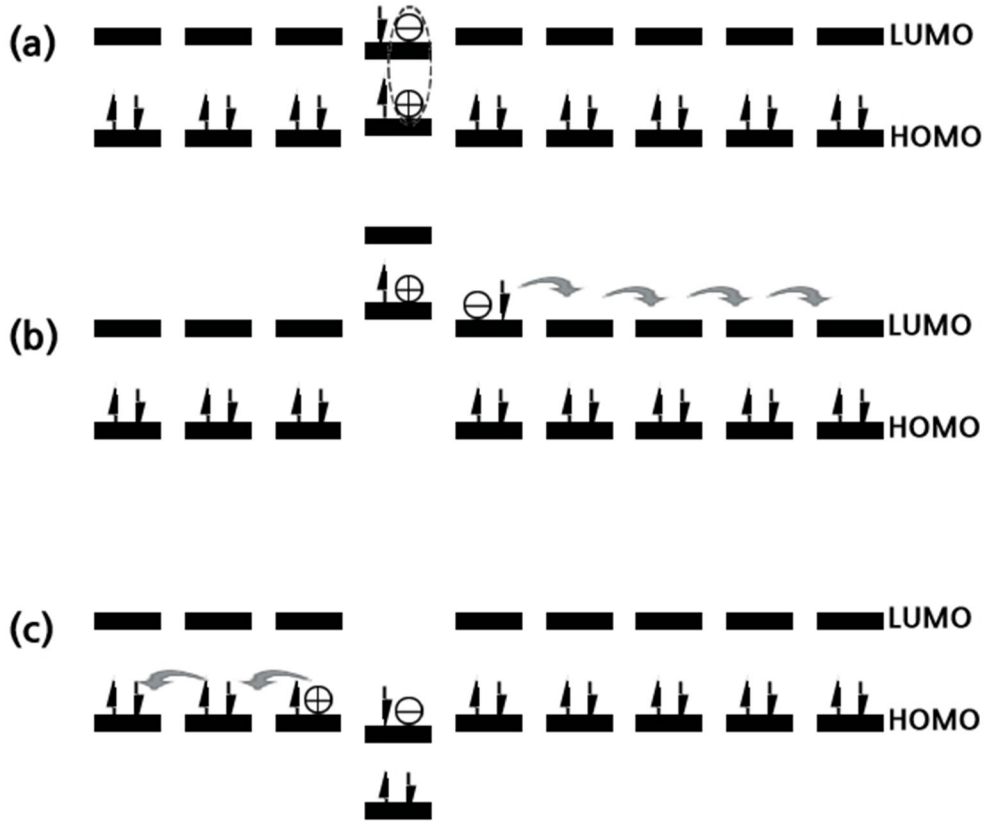

Figure 1.4 Frontier orbital and electron transfer schemes of conjugated polymers in pure (intrinsic) form; (b) donor (n-type) doped form; (c) acceptor (p-type) doped form.

The free holes (positive polarons, Figure 1.5(a)), free electrons (negative polarons, Figure 1.5(b)), a number of other key charge carriers in conjugated polymer include mobile positive bipolarons (Figure 1.5(c)), mobile negative bipolarons (Figure 1.5(d)), neutral solitons (Figure 1.5(e)), positive solitons Figure 1.5(f)), negative solitons (Figure 1.5(g)), and energy carrier excition-polarons (Figure 1.5(h)). Except the exciton-polaron (Figure 1.5(h)) that is an energy carrier but not a charge carrier, all other charged or neutral entities can be driven by an applied electric field and therefore called electric carriers, or simply carriers. Specifically, while two polarons of opposite charge can couple and spin-correlate to each other forming an exciton-polaron (Figure 1.5(h), and may subsequently decay to ground state by emitting a photon, a basic mechanism in OLEDs), two polarons of the same charge can also couple and spin-correlate to each other forming a relatively stable bipolaron entity (a quasiparticle) that can diffuse as a charge carrier containing either two positive (Figure 1.5(c)) or two negative Figure 1.5(d)) unit charges. When two polarons are close together, they can lower their energy by sharing the same distortions, which lead to an effective attraction between the two polarons. The correlated two unit charges typically share one orbital in a bipolaron, or remain in two separate orbitals forming a meta-stable polaron-pair. In either case, they are strongly coupled and correlated in

a lower energy state. Similar to a polaron, the frontier orbital levels of a bipolaron (and a polaron-pair) are also within the HOMO/LUMO gap of pristine material, but closer to the center than that of a polaron. Precise definition of a soliton is not easy and it involves substantial mathematics, however, a neutral soliton (Figure 1.5(e)) formation in polyacetylenes may be simplified as due to, for instance, a degenerate ground state structural distortion, or conjugation paring symmetry rearrangement in the polyacetylene backbone, so that one p_z electron of a backbone carbon atom somehow does not participate in the backbone conjugated π bands formation, thus generating one mobile soliton carrier (Figure 1.5(e-g)). The positive soliton (Figure 1.5(f)) can be regarded as the neutral soliton (Figure 1.5(e)) losses its electron, and the negative soliton (Figure 1.5(g)) can be regarded as the neutral soliton (Figure 1.5(e)) gained an electron with opposite spin. The bipolaron moves as a unit up and down the polymer chain, and is responsible for the macroscopicaly observed conductivity of the polymer. The formation of solitons and polarons results in lone unpaired electrons left in dangling p-orbitals that when removed (termed oxidation), become positive polaron or radical cations. Likewise, the addition of electorons (termed reduction) results in negative polarons or radical anions. The removal or addition of two electrons creates a bipolaron-a.k.a. a radical dication or dianion. Retainment of charge neutrality requires that ions of the opposite charge be nearby.

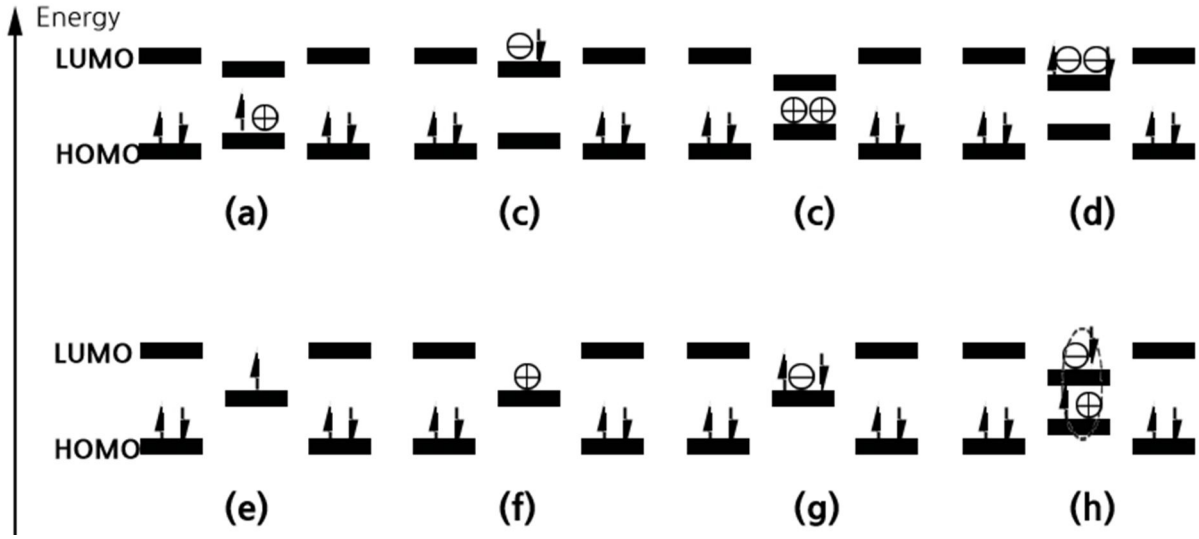

Figure 1.5 Orbital levels schems of carriers: (a) positive (hole) polaron; (b) negative (electron) polaron; (c) positive (hole) bipolaron; (d) negative (electron) bipolaron; (e) neutral soliton; (f) positive (hole) soliton; (g) negative (electron) soliton; (h) excition-polaron.

1.2.3 Conductivity in conjugated polymers

Figure 1.6 shows electrical conductivity of some representative materials at room temperature. It can be seen that either insulator ($\sigma < 10^{-7}$ S/cm), semiconductor ($10^{-7}\,\mathrm{S/cm} \leq \sigma \leq 10^{2}\,\mathrm{S/cm}$), or conductor ($\sigma > 10^{2}\,\mathrm{S/cm}$) may be obtained from conjugated polymers.

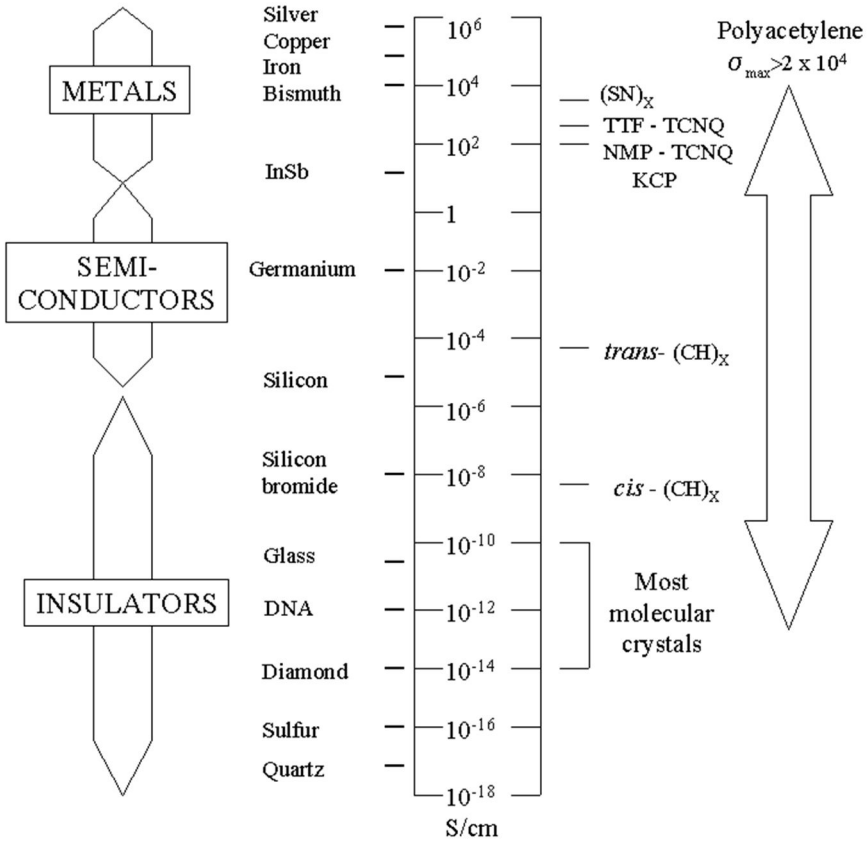

Figure 1.6 Room temperature conductivity of various materials.

1.3 Optical properties

Determined by incoming frequency, most interactions manifest themselves through electron excitation, bond deformation and rotational motion. In conjugated polymers, light with energy ranging from 1-4 eV-approximately equivalent to their band gap energy-excites electronic transitions. The excited molecule releases the energy absorbed non-radiatively through photon emission. For conjugated polymer, the band gap energy, taken to be the onset of the absorption peak in experimentally measured spectra, is related to the amount of overlap between adjacent molecules thus to the conjugation length of the molecule. Thus, shorter conjugation lengths result in bluer absorption

and larger bandgaps. Conjugation lengths vary because of defects in the polymer chain, giving rise to broadened optical spectra. Figure 1.7 graphically describes the absorption and emission process in these materials using Morse potential curves of diatomic molecules. At room temperature, a photon is absorbed from the lowest vibrational level in the ground state to a vibrational level in the excited state. The excitation relaxes quickly ($\sim 10^{-12}$ s) down to the lowest vibrational level in the excited state and from lowest excited singlet state (Kasha's rule), more slowly de-excitates down to vibrational level at the ground state. Because there is the difference in intermolecular distance between the minimum potential energy for the ground and excited states and the transitions are fast enough to be represented by vertical lines (Frank-Condon effect), the emission wavelength will be red shifted from the absorption wavelength. The difference in wavelength between the emission and absorption peaks is called the Stokes shift. The conjugation length of the polymer and the shape of the potentials determine the spectral shape and overlap of the absorption and emission spectra. Absorption spectra are useful for observing the first excited states while emission spectra permit observation of the ground state vibrational levels.

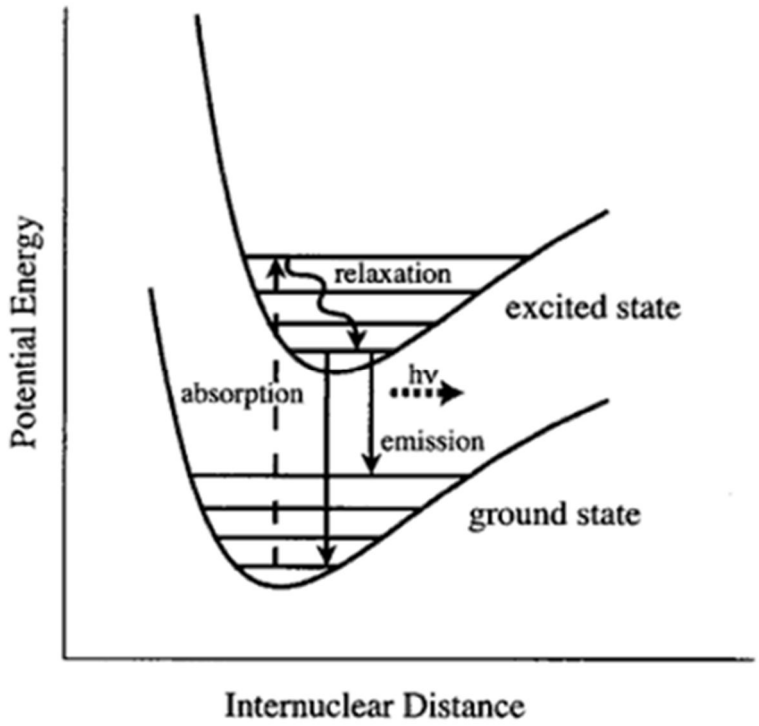

Figure 1.7 Morse potentials for the ground and excited states of a diatomic molecule depicting absorption and emission processes.

1.4 Organic based light-emitting diodes (OLEDs)

1.4.1 Principle of OLED

Commonly researched forms of luminescence in conjugated polymers are photoluminescence-luminescence (PL) by a molecule excited by light and electroluminescence (EL) denoting luminescence by a molecule excited electrically. OLEDs are double charge injection devices, requiring the simultaneous supply of both electrons and holes to the emissive polymer sandwiched between two electrodes.

In electroluminescence, electrons with negative charge and holes with positive charge that have been injected from the cathode and from the anode respectively form a bound state referred to as exciton. Light emission is due to the recombination of the holes and electrons. At low bias, the electron distribution concentrates near the cathode, while the hole distribution is more extend from the anode due to the higher mobility. Thus, most of the recombination takes place near the cathode. As the bias increases, the electron distribution becomes more extended, and the recombination moves from the cathode toward the anode. Operation mechanism has been revealed to be or an injection type in which light is generated from the electrodes.

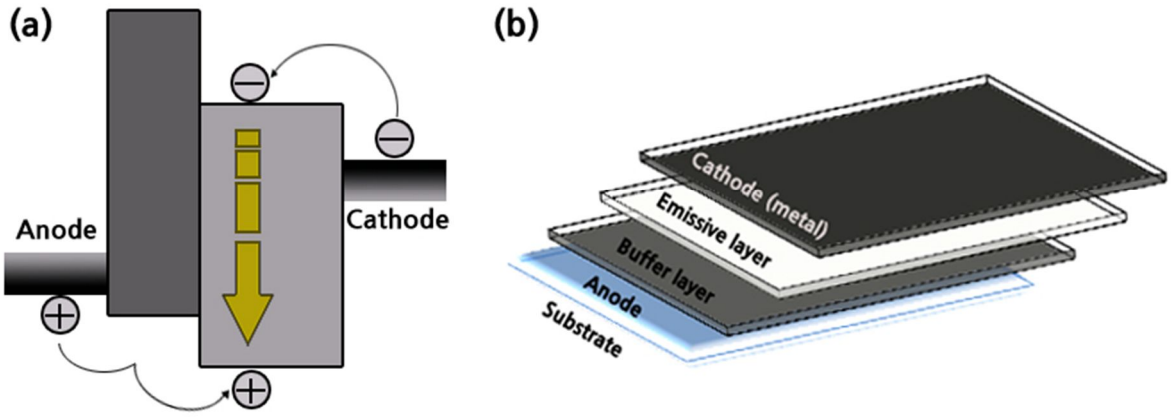

Figure 1.8 (a) Schematic illustration of (a) operation of double-layer OLED and corresponding (b) device configuration.

The use of two or more different materials to perform the required functions of efficient light emission and good charge carrier injection/transport properties in an OLED has resulted in orders of magnitude improvement in device performance. Figure 1.8 shows the structure of OLED and operation mechanism.

1.4.2 Charge transport

Inorganic semiconducting materials such as doped silicon have period structures, the band model applies, and there is delocalization of electrons in the electron conduction band and holes in the valence band. Amorphous organic materials have charge localized in the form of radical ions which move by hopping from molecular site to molecular site. This process is intrinsically less efficient than in the inorganic semiconductors, which is reflected in the lower mobility of charge carriers. Even if the number of injected electrons and holes is same, the mobilities of these carriers may still be different. This may lead to non-radiative recombination of holes and electrons (near the interface between metals and organic semiconductors) and as a consequence, to a low light emitting efficiency and a high driving voltage. Impurities normally act as traps for charge carriers rather than as sources of charge carriers. For example, PPV fabricated via a special precursor route turned out to be p-doped with doping concentrations in order of 10^{17} cm^{-3}. In that case, a Schottky-type depletion zone can be established near a metal contact. However, in vast majority of case, the concentration of impurities is small enough not to perturb the electric field distribution inside a solid-state sample. In such cases, the dark electrical conduction is very low, and the solids are considered as good insulators. Such solids can be made to conduct a relatively large current if the contacts permit the introduction of an excess of free carriers in them. If the carrier enters through a surface boundary, the process is referred to as charge injection. The charge injected conduction is governed by charge injection barriers at the electrode contacts and charge transport properties of materials. Depending on the charge injection efficiency and mobility of charge carrier, the current is either space-charge-limited current (SCLC) or injection-limited current (ILC).

For a perfectly ordered or disordered insulating material, or those containing very shallow traps, the SCLC in a sample of thickness d obeys Child's law:

$$J_{SCLC} = \frac{9}{8}\varepsilon_o\varepsilon\mu\frac{F^2}{d}$$

In the presence of discrete traps

$$J_{SCLC} = \frac{9}{8}\varepsilon_o\varepsilon\Theta\mu\frac{F^2}{d}$$

where

μ is the microscopic mobility of the carriers

ε is the dielectric constant

ε_o is the permittivity in vacuum

Θ is the fraction of free (n_f) to trapped (n_t) space-charge

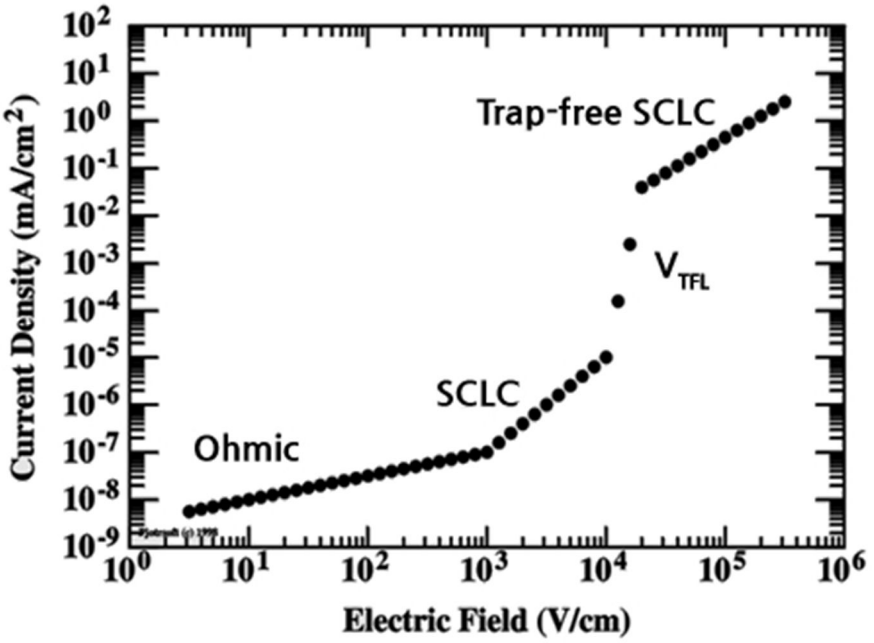

Figure 1.9 Schematic graph showing current density (J) verse voltage (V) for an insulator with single energy traps.

1.4.3 Charge injection

The operation voltage and the charge injection energy barrier of the PLED devices depend on the work function of the electrode materials and the electronic energy levels of the HOMO and LUMO of the conjugated polymers. Injection of holes and electrons into the emitting material and their subsequent radiative recombination constitutes the operation mechanism of a PLED. For successful injection, the electrode work function must be properly matched. This is one of the limiting factors of PLED as metal cathodes with low enough work functions for electron injection, such as calcium, are reactive with the environment. In order to be injected from the electrodes, the charges must surmount or tunnel through a barrier at the polymer/electrode interface, which is determined by the position of the HOMO, or π orbital, and the LUMO, or π^* orbital, and the position of the electrode metal work functions.

The low charge carrier concentration is swept out by built-in field that arises from the difference in

work functions of the two electrodes. The electronic structure of the LED can be approximated by the rigid band model. The built-in field causes the uniform slope in the energies of the states in the bulk of the conjugated polymer; there is negligible band bending. When a positive bias is applied to the LED, the Fermi level of the cathode is raised relative to that of the anode. Thus, the thickness of the barrier is a function of the applied voltage; the barrier thickness decreases as the voltage is increased. Carriers tunnel through the barrier primarily by Fowler-Nordheim field emission tunneling from the anode and cathode into the π band, and the π^* band. Consequently, the electronic structure of the LED can be approximated by the simple band model displayed in **Figure 1.10.**

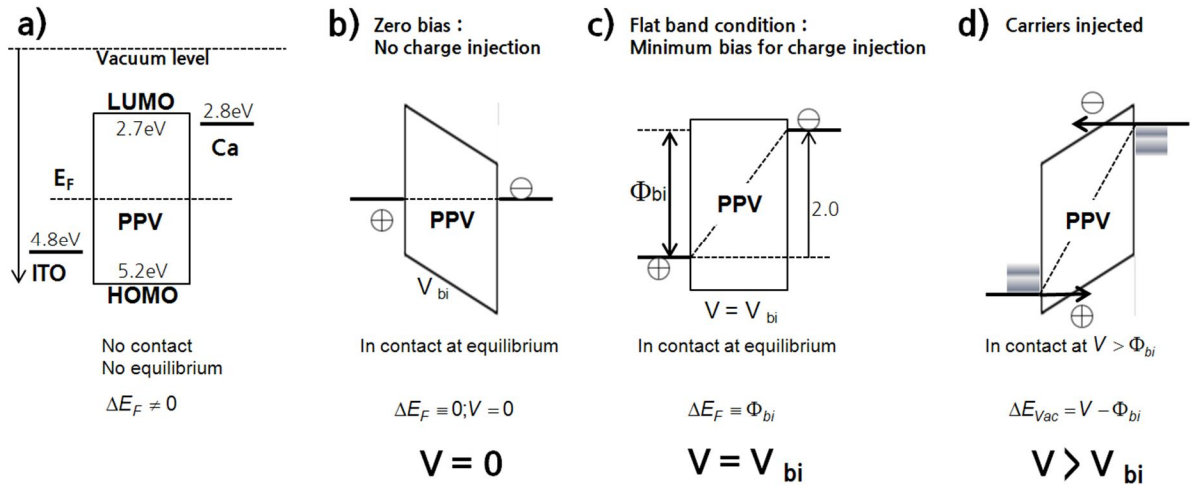

Figure 1.10 The electronic structure of the LED. (a) Before contact between electrode and semiconducting polymer. (b) Zero bias with a common Fermi level across the device (note that within the semiconducting polymer layer, the Fermi level moves across the energy gap on going from the anode to cathode) (c) Flat band condition occurs when the applied voltage equals the difference in the work functions of the anode and cathode. This is the minimum voltage required for injection of electrons and holes. Ideally, the electroluminescent emission should turn on at this voltage. (d) Forward bias; carriers are injected through the triangular barrier at the anode (holes) and cathode (electrons) and meet within the polymer film where they radiatively recombine (electroluminescence).

When a positive bias is applied to the LED, the Fermi level of the cathode is raised relative to that of the anode, as shown in Figure 1.10 (d). Thus the thickness of the triangular tunneling barrier is a function of the applied voltage; the barrier thickness decreases as the voltage is increased. Carriers tunnel through the barrier primarily by Fowler-Nordheim field emission tunneling from the anode and cathode into the semiconducting polymer. Thermionic emission over the barriers can also play a role if the barriers are small and the temperature is relatively high. Since the rate of injection by Fowler-Nordheim tunneling is determined by the strength of the electric field, it is important for the polymer

layer to be thin so that high electric field can be obtained at low voltages.

To optimize the performance of polymer LEDs, it is important to minimize the barriers for charge injection by choosing electrodes with work functions that are well matched to the bands of the polymer. But, if one carrier type is injected much more efficiently and drifts in the applied electric field with higher mobility than the other, then many of the majority carriers will traverse the entire polymer layer without recombining with a minority carrier. Thus, maximum efficiency can be achieved only through balanced electron and hole currents.[27]

1.4.4 Device efficiency in OLED

The EL efficiency is crucial factor for the development of OLEDs. Three well-known factors which influence EL efficiency in light-emitting diodes are: (1) the balanced injection, which is a function of barrier height between the emissive layer and the respective electrodes. Hole and electron conduction occur in opposite directions and do not occur at the same rate. In general, electron mobility is a slower process than hole transport. Thus, bipolar transport of the charge carriers also has responsibilities of improving device efficiency. (2) exciton formation within the chromophore, which is a function of the confinement of injected charge carriers; and (3) the radiative decay of excitons, which depends on the photoluminescent (PL) efficiency of the chromophore. Since Frenkel excitons have been found to be the pertinent species in OLEDs/PLEDs in which electrons and holes are tightly paired, there is an implication that injected charge carriers need to be confined in the smallest achievable volumes to form such exciton with high probability and hence to maximize EL efficiency.

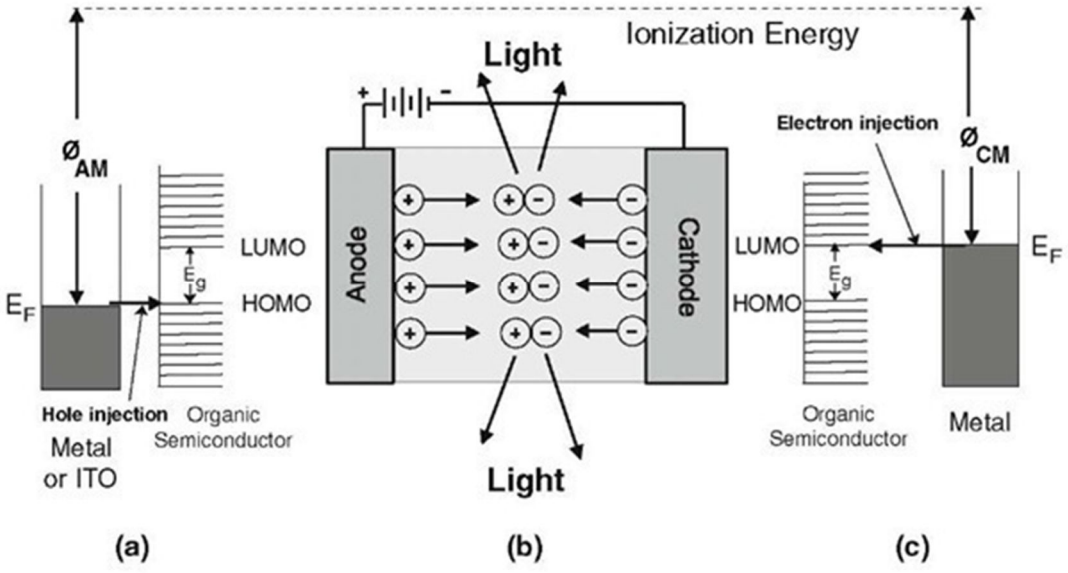

Figure 1.11 Schematic representation of a single-layer organic light emitting diode. (a) A metal "band diagram" adjacent to HOMO/LUMO levels of an organic semiconductor is depicted. (b) Schematic functioning of a single layer OLED. (c) HOMO/LUMO levels and metal "band diagram" for electron injection.

The internal quantum efficiency η_{int} of an OLED is defined as the ratio of the total number of photons produced within the device to the number of electrons flowing in the external circuit or

$$\eta_{int} = \frac{\#\text{ of photons emitted from active region per second}}{\#\text{ of electrons injected into OLED per second}}$$

Similarly, external quantum efficiency η_{ext} is defined as

$$\eta_{ext} = \frac{\#\text{ of photons emitted into free space per second}}{\#\text{ of electrons injected into OLED per second}}$$

The external quantum efficiency gives the ratio of usable photons emitted out of the device to the number of injected electrons.

$$\eta_{ext} = \eta_{int}\eta_{ph} = \gamma\eta_{ex}\Phi_p\eta_{ph}$$

where η_{ph} is the light out-coupling efficiency, η_{ex} is the fraction of total excitons formed which result in singlet excitons (from spin statics, $\eta_{ex} \sim 1/4$ for fluorescent molecular dyes, and 1 for phosphorscent materials), γ is the electron-hole charge balance factor or in other words, the fraction of injected charge carriers forming excitions, and Φ_p is the quantum yield (the photoluminescence efficiency) of the dopant. Because only singlets are radiative in fluorescent material, $\eta_{ex} \sim 1/4$, η_{ext} is limited to 5%, assuming $\eta_{ph} \sim 1/2n^2 \sim 20\%$ for a glass substrate with index of refraction n=1.5. In contrast, both singlet and triplet can be radiative by using high efficiency phosphorescent materials, and η_{int} can approach 100%, in which case $\eta_{ext} \sim 20\%$ can be expected. External quantum efficiency is commonly calculated from experimental data by

$$\eta_{ext} = \frac{5.0\times10^3}{(hv)\varphi(\lambda)}\text{LE}$$

where LE is the luminous efficiency, hv is the photon energy (in eV) of the emission and $\varphi(\lambda)$ is the photonic luminosity function.[28]

1.5 Hybrid organic-inorganic polymer light emitting-diodes (HyPLED)

1.5.1 Inverted structure in PLEDs

OLED displays can use either passive-matrix (PMOLED) or active-matrix(AMOLED). Active-matrix OLEDs (AMOLEDs) require a thin-film transistor backplane to switch each individual pixel on or off, but allow for higher resolution and larger display sizes. Display Search forecasts the total OLED display market will grow to $6.2 billion by 2016 from $0.6 billion in 2008.

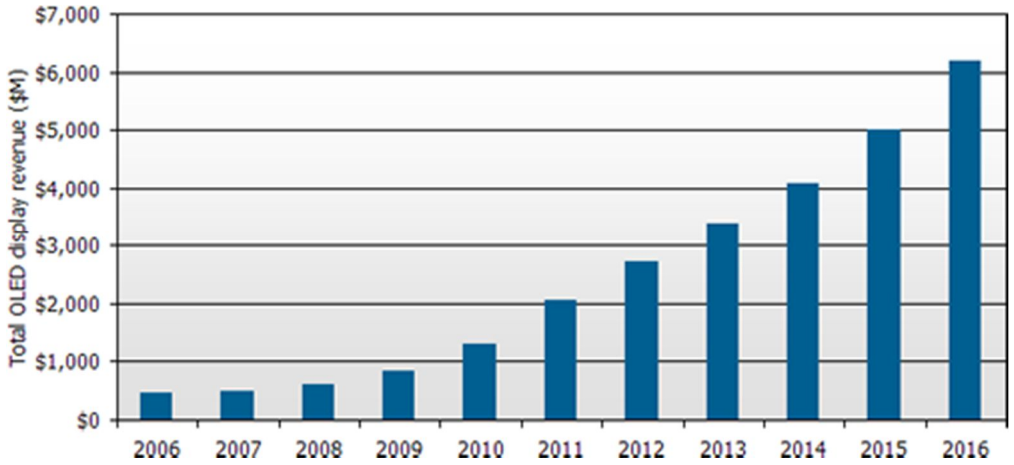

Figure 1.12 OLED display revenue forecast

Bottom emission devices use a transparent or semi-transparent bottom electrode to get the light through a transparent substrate. Top emission devices[29] use a transparent or semi-transparent top electrode emitting light directly. Top emitting OLEDs are better suited for active-matrix applications as they can be more easily integrated with a non-transparent transistor backplane. In contrast to a conventional OLED, in which the anode is placed on the substrate, an inverted OLED uses a bottom cathode that can be connected to the drain end of and n-channel TFT especially for the low cost amorphous silicon TFT backbone useful in the manufacturing of AMOLED displays.[30]

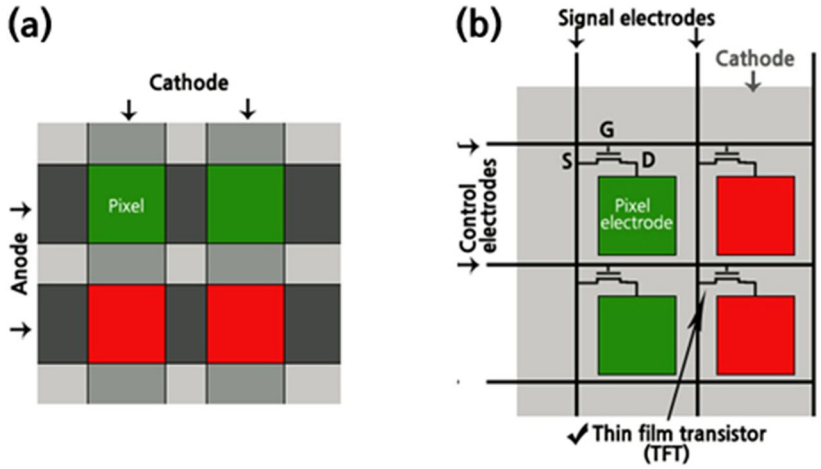

Figure 1.13 (a) Passive and (b) active matrix OLED.

1.5.2 Hybrid organic-inorganic polymer light emitting-diodes (HyPLED)

Recently transition metal oxides (TMO) have been employed as charge transport and particularly as electron injection layers in hybrid organic-inorganic light emitting diodes (HyLEDs), demonstrating the possibility to prepare air-stable electroluminescent devices. Limitation of conventional structure of PLEDs is the requirement for a low work function, air-sensitive metal cathode such as calcium and magnesium or charge injecting material. They require rigorous encapsulation to ensure device lifetime.

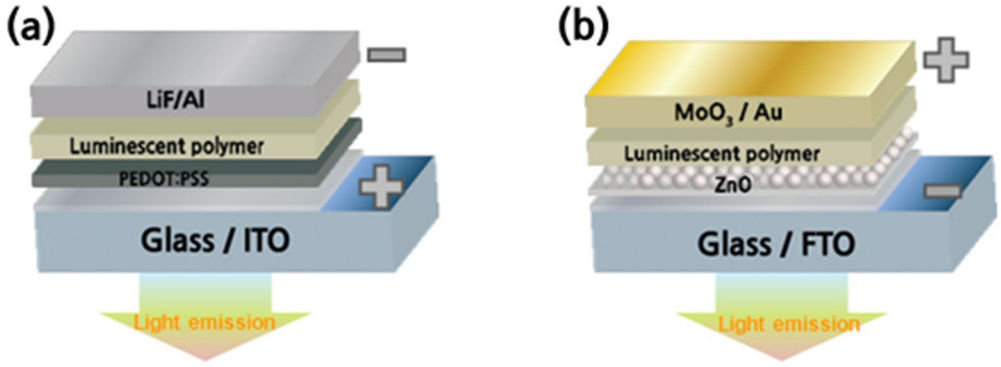

Figure 1.14 Device configuration of (a) conventional and (b) inverted structure.

Inverted structured PLEDs should not require the use of low work function metal. This configuration has an air-stable transition metal oxide (TMO) layer having possibility of solution processing such as TiO_2, ZnO, HfO_2, and ZrO_2 and the hole injection layer (HIL) such as MoO_3.[31-35] These layers act as a hole blocking electron injection layers (EIL) as well as an exciton confinement layer

Cs_2CO_3 has been deposited as a secondary electron injection and hole blocking layer on top of the

inorganic metal oxide layers.[36,37] The preparation of such devices consists of low-cost solution processable deposition of a thin metal oxide film on top of the transparent electrode, followed by the spin-coating of the light emitting polymer (LEP) and the deposition of a high work function metal. Inorganic metal oxide cathodes like titanium oxide (TiO_2) and Zinc oxide (ZnO) provide favorable properties like good mechanical and compositional stability, transparency, good electrical conductivity, and easy deposition with great control on the film morphology.[38,39]

HyPLEDs have a unique hole-dominated operating mechanism: initially holes are efficiently injected into the LEP through a molybdenum oxide (MoO_3) layer placed in between the polymer and the anode.[36,40] Thus, holes with positive charge accumulate at the metal oxide-polymer interface creating a strong interfacial field that assists the electron injection.

1.5.3 Interfacial engineering in HyPLEDs

To enhance the device performances, the additional dipole layers metal/polymer or metal oxide/polymer interface play a functional role by blocking injected carriers from traversing the structure and reaching the other contact without recombining. Moreover, they faciliate carrier injection into emissive layer by reducing contact barrier and recombination probability by blocking the charge carriers from counter electrode.

1.5.3.1 Self-assembled dipole molecules (SADMs)

The magnitude and orientation of the dipole moment of self-assembled dipole molecules (SADMs) influence the work function of adjacent layer, herein ZnO. As a consequence, the charge injection barrier between the conduction band of the ZnO and could be efficiently controlled resulting that electron injection efficiency is remarkably enhanced. The HyPLEDs modified with a negative dipolar SADM exhibited enhanced device performances, which correspond to approximately a fourfold compared to those of unmodified HyPLEDs.

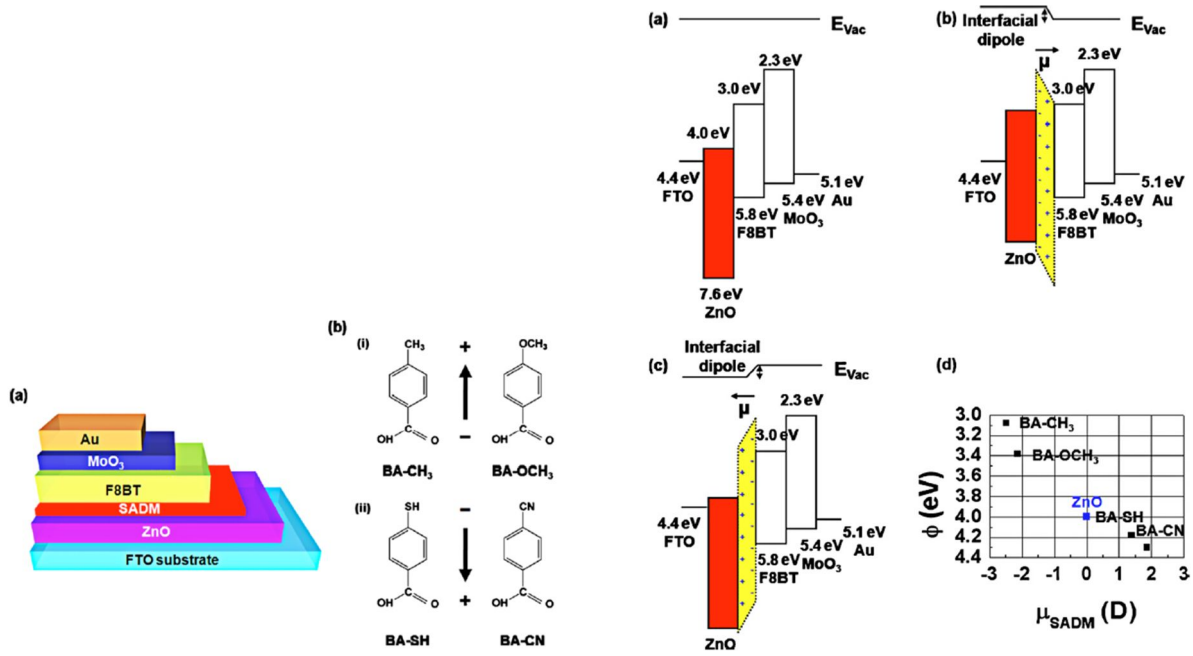

Figure 1.15 (a) Device architecture of single F8BT layer HyPLEDs with SADMs on a ZnO surface. (b) Chemical structures of carboxylic acid based SADMs: (i) negative dipole molecules (ii) positive dipole molecules. Schematic energy diagrams for flat band conditions of HyPLEDs with (a) unmodified ZnO, (b) negative, and (c) positive SADM modified ZnO. (d) Experimentally measured work functions of ZnO as a function of the _SADM using UPS.[41]

Table 1.1 Detailed device characteristics of HyLEDs with or without SADM modification of ZnO.[41]

Device configuration	L_{Max} (cd/m^2) (@ voltage)	LE_{Max} (cd/A) (@ voltage)	$V_{turn-on}$ (V)
FTO / ZnO (80 nm) / F8BT (250 nm) / MoO_3 (10 nm) / Au (65 nm)	**11,000 (9.4 V)**	**0.7 (8.0 V)**	**2.4**
FTO / ZnO / BA-CH_3 / F8BT / MoO_3 / Au	**38,000 (9.8 V)**	**2.8 (9.6 V)**	**2.2**
FTO / ZnO / BA-OCH_3 / F8BT / MoO_3 / Au	**38,200 (10.4 V)**	**2.1 (10.0 V)**	**2.4**
FTO / ZnO / BA-SH / F8BT / MoO_3 / Au	**200 (8.8 V)**	**0.01 (8.6 V)**	**4.0**
FTO / ZnO / BA-CN / F8BT / MoO_3 / Au	**15 (7.6 V)**	**0.001 (6.8 V)**	**4.6**

1.5.3.2 N-type metal oxide/conjugated polyelectrolyte hybrid charge transport layers

An interfacial engineering strategy employing n-type–metal oxide/conjugated polyelectrolyte (CPE) hybrid charge-transport layers was demonstrated for highly efficient polymer light-emitting diodes (PLEDs). The hybrid metal-oxide/CPE layer facilitates electron-injection, while blocking hole-transport, and thereby maximizes electron-hole recombination within the emitting layer. A series of metal-oxide/CPE combinations were tested in inverted PLEDs (FTO/metal-oxide/CPE/F8BT/MoO3/Au). Specifically, HfO_2/CPE double layer achieved an electroluminescence (EL) efficiency of up to 25.8 cd/A (@ 6.4 V, one of the highest values reported for fluorescent PLEDs).

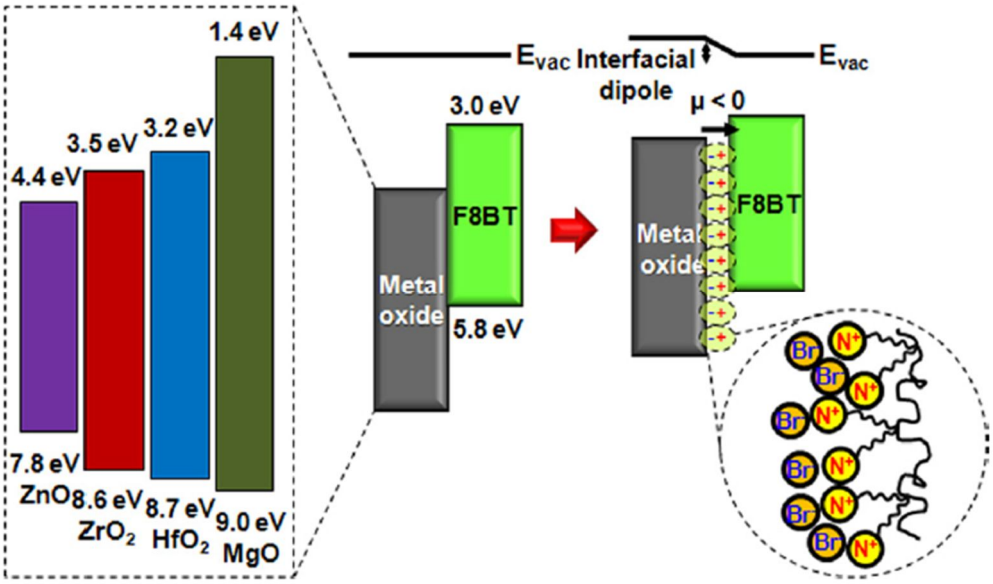

Figure 1.16 Schematic energy-level diagrams at the n-type-metal-oxide/F8BT junction with and without the CPE having negative dipoles.[42]

Table 1.2 Detailed device characteristics of inverted PLEDs with various interfacial charge-transport layers.[42]

Device configuration	Bias @ 1000 cd/m^2	$\eta_{EL,\ max}$ (cd/A) @ bias	$\eta_{EL,\ max}$ (lm/W) @ bias
ZnO	7.8 V	2.2 @ 10.4 V	0.7 @ 10.4 V
ZrO_2	13.4 V	5.6 @ 13.8 V	1.3 @ 13.8 V
HfO_2	8.4 V	5.5 @ 9.2 V	1.9 @ 8.8 V
MgO	15.4 V	2.9 @ 14.8 V	0.6 @ 14.8 V
ZnO/CPE	7.8 V	11.9 @ 9.4 V	10.1 @ 9.4 V
ZrO_2/CPE	8.4 V	15.8 @ 7.6 V	6.8 @ 7.2 V
HfO_2/CPE	7.4 V	25.8 @ 6.4 V	12.6 @ 6.4 V
MgO/CPE	17.4 V	7.7 @ 7.6 V	3.2 @ 7.6 V

1.6 Experimental

1.6.1 Device fabrication

PLEDs were fabricated on indium-tin-oxide (ITO) or fluorine-tin-oxide (FTO) coated glass substrates. In our study on conventional PLED configuration, ITO is used as anode. As cathode electrode, FTO with transparent ZnO layer was used in inverted PLED configuration. The additional layer of organic/inorganic layer is deposited between electrode and emissive layer to act as carrier injection/transport layer. Solution processing such as spin-coating and spray pyrolysis method were used for deposition of organic or inorganic material. The device fabrication was completed by thermal evaporation of diverse metal electrode under vacuum at a base pressure of 2×10^{-7} Torr. Several methods to form a thin film are shown as follows:

1) Spin coating method: An excess amount of the solution is dropped on the substrate, which is then rotated at high speed in order to spread the solution by centrifugal force. The film thickness can be adjusted by varying the rotation speed, the rotation time, and the concentration of the used solution.

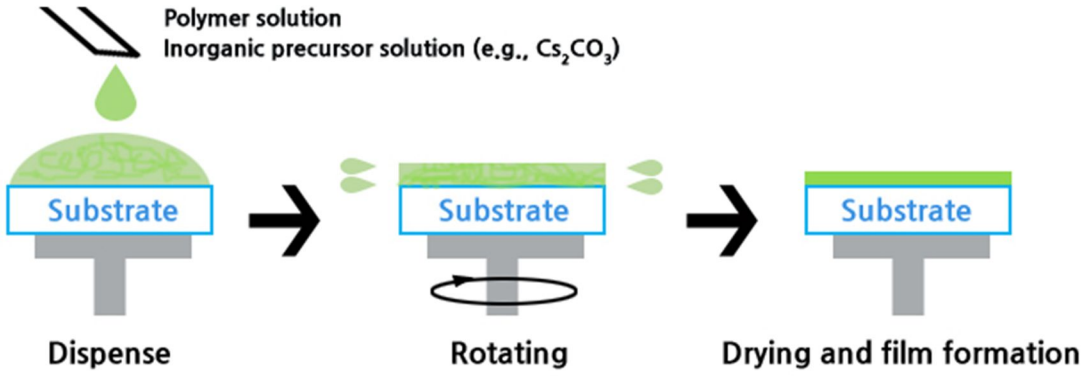

Figure 1.17 Illustration of spin-coating processing

2) Spray pyrolysis

The precursor solution is supplied with high-purity oxygen gas (carrier gas) onto hot substrate (above 400℃) on which the film is to be grown. In order to ensure a homogeneous pyrolytic reaction on the hot substrate, the heater is moved back and forth perpendicularly to the spraying nozzle.

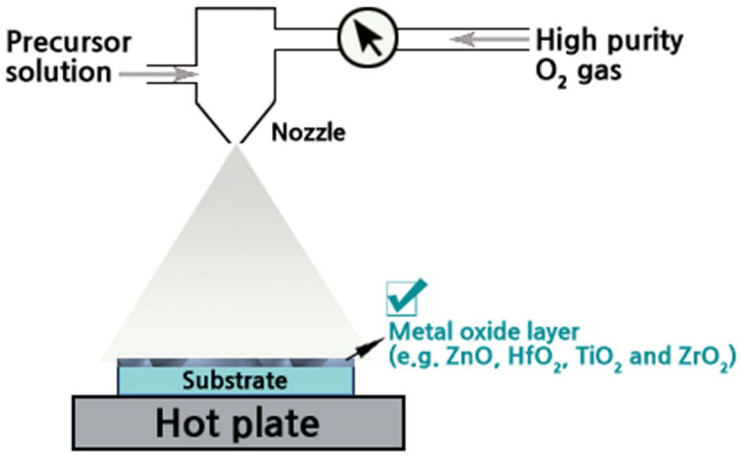

Figure 1.18 Schematic of the spray pyrolysis process

1.6.2 Measurement of device performance

A convenient configuration for measuring luminous efficiency from PLEDs is shown in Figure 1.18. The device performances were measured using a Keithley 2400 source measurement unit and a Konica Minolta spectroradiometer (CS-2000) in atmospheric conditions.

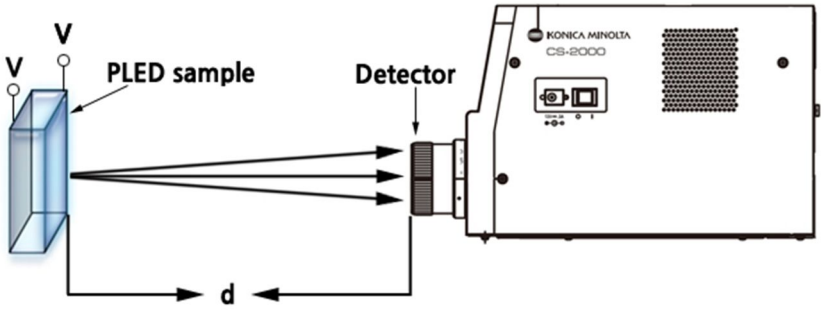

Figure 1.19 The configuration for measuring PLED luminous intensity

Chapter 2 Luminescent polymer and ionic liquid blends: Polymer light-emitting electrochemical cells (PLECs)

2.1 Objective and overview of the research

Great attention has been paid to organic/polymer based light-emitting diodes (LEDs) over the past two decades for solid-state lighting, flat-panel display, and flexible electronic devices.[1] For commercially applicable LEDs, high device efficiency and stable lifetime of organic/polymer light emitting diodes are necessary. Recently, hybrid organic-inorganic polymeric light-emitting diodes (HyPLEDs) with metal oxides (ZnO, TiO_2, ZrO_2, and MoO_3) as a charge injection layer have been proposed due to the excellent air stability and high device performance that results from their use.[31,33,34,43-45] However, these HyPLEDs have intrinsic limitations in producing high device efficiency because of unbalanced charge carrier injection and transport. It has recently been reported that MoO_3 shows ohmic hole injection into materials with ionisation potentials significantly deeper than that for poly (9,9′-dioctylfluorene-co-benzothiadiazole) (F8BT).[46] MoO_3 has also been used in organic thin-film transistors (OTFTs)[47], organic LEDs[48], and HyPLED applications for improved hole injection. However, at the interface between the conduction band of ZnO (~ 4.0 eV) and the lowest unoccupied molecular orbital (LUMO) of an active layer there exists a large energy barrier (more than 1 eV) in HyPLEDs, which results in poor electron injection efficiency and finally brings serious problems in obtaining highly efficient HyPLEDs.[33,35] Therefore, interfacial engineering between the organic semiconductor and the inorganic layer is needed to reduce the barrier and balance the charge carrier injection to allow for low operating voltage and high device efficiency. Several methods have been suggested to address this problem: introducing cesium carbonate (CS_2CO_3),[36,37] lithium fluoride,[49] conjugated polyelectrolytes,[50] ionic liquid,[51] or a self-assembled dipole monolayer (SADM)[41,52,53] between contact layers can reduce the injection barrier, balance the charge carrier injection, and improve the device performance. However, there is still considerable room for optimizing contacts so as to yield high device performance.

Here, we present a straightforward strategy to reduce the charge injection barrier and enhance device efficiency. This method relies on the mixing of mobile ionic liquid molecules (ILMs) into the fluorescent polymer layer in hybrid organic-inorganic polymeric light-emitting electrochemical cells (HyPLECs).

2.2 Research background

2.2.1 Polymer light-emitting electrochemical cells (PLECs)

The combination of reversible electrochemical doping and optoelectronic properties of conjugated polymers enable the creation of the solid state polymer light-emitting electrochemical cells (PLECs). The conjugated polymer in LEC is doped to create a p-n junction by electrochemical doping. Doping serves to shift the electrochemical potential of the polymer, thereby making possible polymer p-n junctions. A typical LEC consists of an emitting layer of a polymer blend (conjugated polymers + ion supply materials) sandwiched between two electrodes. Figure 2.1 shows a schematic of the LEC structure in which ion salt are incorporated in luminescent polymer matrix as emitting layer. A blend solution is made by co-dissolving the luminescent polymer and ionic liquid molecules (ILMs) in a common solvent. LECs are fabricated by relatively simple processing steps, an advantage which is a more general feature of polymer semiconducting devices.

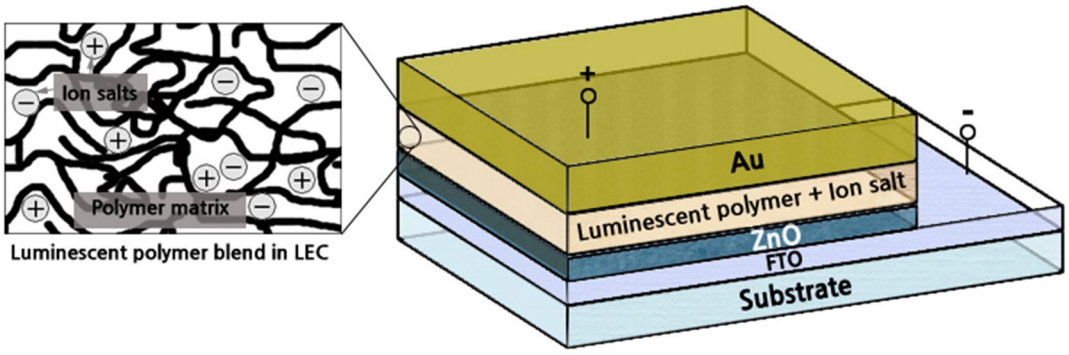

Figure 2.1 Device architecture of an LEC used in this study

2.2.2 LEC operating mechanism

The operating mechanism of the light-emitting electrochemical cells (LECs) is different from that of LEDs[53-56] as depicted in Figure 2.2. At zero bias, the semiconducting polymer is in the undoped state. When a voltage greater than the energy gap of the polymer is applied to the metallic contacts, the ions redistribute to each electrodes. The mobile anions and cations accumulated at each electrode/active layer interface under an applied bias form electric double layer and then a light-emitting p-n junction in emissive polymer layer. This p-n junction effectively reduces the charge injection barriers at the electrode/active layer interfaces, balanced charge injection, and high electroluminescence efficiency at relatively low operating voltages.

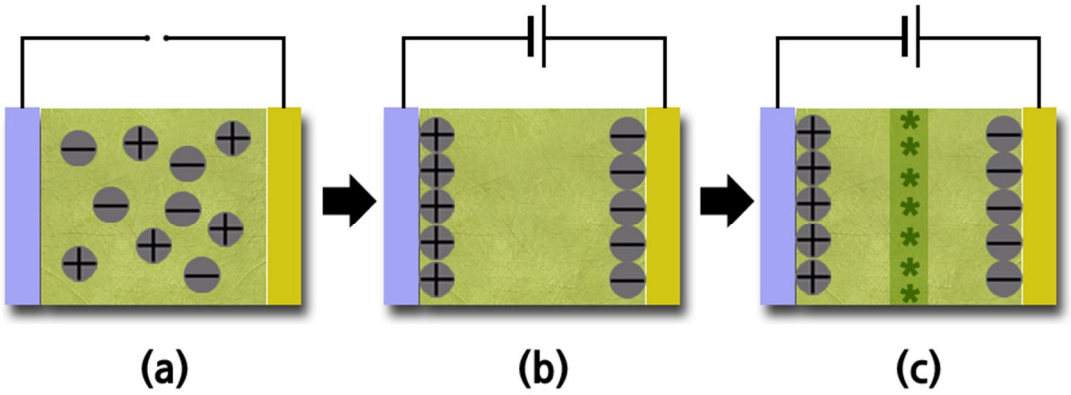

Figure 2.2 Schematic representation of polymer LEC operation (a) before and (b) under an applied forward bias. (c) The recombination of injected electrons and holes in emissive layer caused by the redistribution of anions and cations.

As mentioned before, HyPLECs and HyPLEDs show different operating mechanism. When a bias is initially applied, the electric field is equally distributed across the device, as shown in Figure 2.2 (a). An applied bias causes the motion of anions and cations toward the Au anode and the FTO/ZnO or FTO cathode, respectively, and the movement of the ions creates double layers, giving rise to then a light-emitting p-n junction in emissive polymer layer at each electrode/active layer interface until steady-state is reached, as shown in Figure 2.2 (b) This p-n junction enhances the charge carrier injection, thereby eliminating the restrictions on the work function of each electrode. Therefore, the HyPLECs exhibit extremely low turn-on, and high luminance efficiency at low operating voltage without matching the work functions between each electrode and active layer.[57,58]

Two models for device operation have been proposed[59]: an electrochemical model from which the devices get their name and an electrodynamic model. In the electrochemical model (Figure 2.3 (a)), injection of charge carriers (electrons and holes) results in the formation of highly conductive p- and n-doped regions adjacent to the anode and cathode, respectively. These doped layers facilitate the injection of further charges, causing the contacts to become highly conductive (that is, they become 'ohmic') regardless of the electrode work functions. The p- and n-type regions meet in the bulk of the device to form an undoped '*in situ*' p–n junction where the electrons and holes recombine radiatively. Owing to the high conductivity of the doped layers, the electric field is small throughout the doped regions and the externally applied potential difference is therefore dropped across the central junction, leading to a high electric field in the middle of the device. In the electrodynamic model (Figure 2.3 (b)), an applied bias causes the anions and cations to drift towards the positive and negative electrodes, respectively. Owing to the high density of ions, small movements of the ions give rise to very large

electric fields, and the ions continue to redistribute in the bulk until steady-state is reached and the local electric field has been cancelled throughout the bulk. A large electric field can only be sustained at the contacts where the motion of the ions is blocked by the electrodes. Hence, the electric potential is dropped across thin interfacial layers close to the electrodes, and the electric field is almost zero everywhere else. The high fields at the electrodes facilitate the injection of charges, thereby removing the restrictions on electrode work function that apply to conventional OLEDs. An important difference between the two models is the distribution of the internal electric field. The electrochemical model predicts a large electric field in the central junction and a small field through the rest of the film, whereas the electrodynamic model predicts high electric fields close to the contacts with the bulk being virtually field-free.

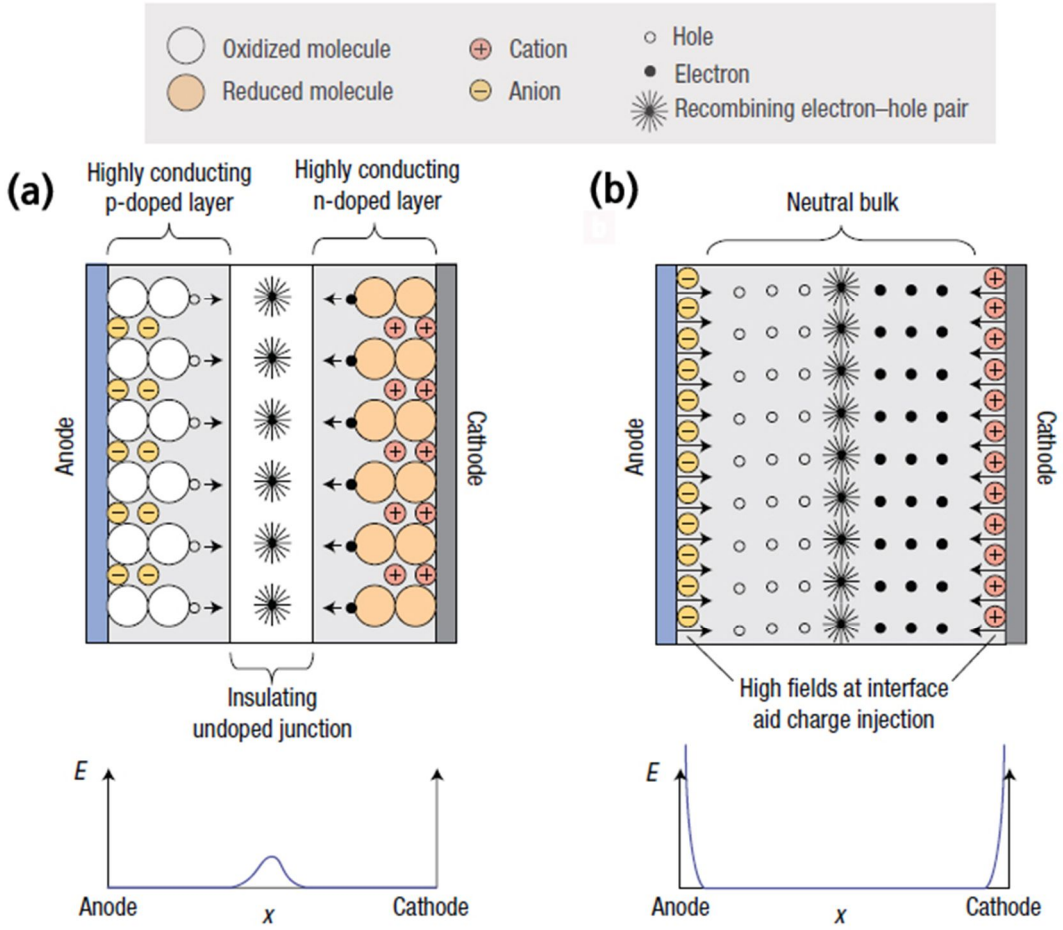

Figure 2.3 The two models proposed for LECs operation with associated spatial distribution of the electric field shown underneath. (a) The electrochemical model. Injection of holes and electrons causes oxidation and reduction of the organic semiconductor close to the anode and cathode, respectively. Counter ions move to compensate the reduced and oxidized molecules, leading to the

formation of p- and n-doped layers that extend into the bulk of the device. The high conductivities of the doped regions cause the electrode/organic interfaces to act as low-resistance contacts, allowing easy carrier injection. The radiative recombination of electrons and holes in the middle of the device depletes the charge carriers, leading to the formation of an undoped junction region across which the entire applied bias is dropped. (b) The electrodynamic model. Under an applied forward bias, a slight redistribution of the ionic charge occurs, leading to an excess of anions and cations at the anode and cathode, respectively. The accumulated ions cause a local enhancement in the electric field and — if the density of ions is sufficiently high — leave the bulk of the device virtually field-free. The electrons and holes diffuse through the field-free bulk and meet in the middle of the device where they recombine.[Reproduced from deMello, John C. 2007, 'Organic electronics: What's in a name?', Nat Mater, vol. 6, no. 11, pp. 796-7.]

2.2.3 LECs vs. LEDs: Advantages and disadvantages[27]

PLEDs are field-driven devices in which the electron and hole currents are limited by carrier injection at the electrode/polymer interface. As a result, PLEDs are characterized by sensitivity to electrode materials (low work function metals are needed for injection of electrons in conventional-type PLEDs) and device thickness. Whereas polymer LECs offer advantages compared with PLEDs as below,

i. Balanced electron and hole currents. Since the doped semiconducting polymer has low resistivity and tends to ohmic contacts with electrodes, more nearly balanced electron and hole injection is expected.
ii. Low operating voltages. The turn-on voltage of an LEC is roughly equal to bandgap of semiconducting polymer (2-3V).
iii. Insensitivity to electrode materials. The charge carrier injection in LECs is not sensitive to the work function of the electrode material.
iv. Insensitivity to film thickness. LECs are voltage-driven devices. The applied bias voltage drops mostly in the more resistive undoped intrinsic region. As a result, the device characteristics of LECs are not sensitive to device thickness.

Unlike an inorganic p-n junction, the p-i-n junction in an LEC is dynamic; i.e. it relaxes by discharging when the externally applied voltage is removed. A new operation requires that the junction is rebuilt before the maximum light output can be achieved. As a result, LECs also have serious disadvantages:

i. Slow response. The light emission turn-on of an LEC is slow because seconds or even minutes are required for the redistribution of ions during the creation of the p- and n-junction.
ii. Poor stability at high operating voltage. When the applied bias exceeds the electrochemical stability window of the system, the device degrades due to ‘overdoping’.
iii. Hysteresis behavior. LECs exhibit hysteresis. The hysteresis is caused by the interplay of the slow ionic processes and the fast electronic processes involved in LEC operation.

2.3 Experimental

Figure 2.4 (a) shows the complete device architecture of HyPLECs. The hybrid devices were fabricated by successive deposition of SnO2:F (FTO) as a transparent cathode, ZnO, a blended active layer, phenyl-substituted poly *para*-phenylene vinylene (PPV) copolymer [SY (Merck Co., Mw =1 950 000 g/mol)]:tetradecyltrihexylphosphonium bis(trifluoromethylsulfonyl) amide (hydrophobic ILMs, Aldrich), and Au as the anode. An 80-nm-thick ZnO film was deposited by spray pyrolysis method onto the precleaned FTO substrate using a ZnO precursor solution of zinc acetate dehydrate (Aldrich) in methanol at 400 °C.[33] A single active layer is spin-coated (1500 rpm, 45 s) from a blend solution (9 mg/ml), which is composed of SY [Figure 2.4 (b)] as luminescent polymer and ILMs [Figure 2.4 (b)] as ion supply in chlorobenzene with different ILMs content, such as 0 (pure SY), 10, 20, 25, and 35 wt %. The blend films were annealed at temperature of 80 °C for 1 h in a nitrogen atmosphere glovebox. A 70-nm-thick Au layer is thermally evaporated on the active layer to complete device fabrication under vacuum at 10^{-6} Torr.

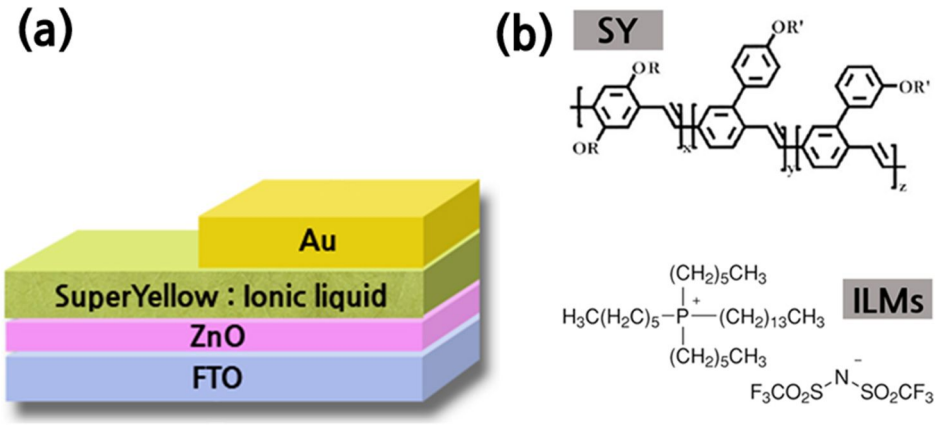

Figure 2.4 (a) Device configuration of HyPLECs using a blend of super yellow (SY) and ionic liquid molecules (ILMs). (b) Chemical structure of phenyl-substituted PPV copolymer, SY as a luminescent polymer and tetradecyltrihexylphosphonium bis(trifluoromethylsulfonyl)amide as mobile ILMs.

The device performances were measured using a Keithley 2400 source measurement unit and a Konica Minolta spectroradiometer (CS-2000) in atmospheric conditions

2.4 Results and discussion

The performance of our HyPLECs was improved from a luminance of 0.11 cd/m^2, luminous efficiency of 0.002cd/A, and turn-on voltage of 34.0 V for pure super yellow (SY) layer to a luminance of 3400 cd/m^2, luminous efficiency of 1.20 cd/A, and turn-on voltage of 2.1 V for blend films by optimizing the composition of SY and ILMs in HyPLECs.

The SY:ILMs blend films were observed by atomic force microscopy (AFM) as shown in Figure 2.5. As the ILMs weight percent was increased in fluorescent SY polymer, the root mean square roughness (RMS) slightly increased. However, polymer blend film containing large ion portion (35 wt %) still had low roughness (0.7 nm), and we could not find a significant phase separation in the blend film of SY and ILMs because hydrophobic ILMs show excellent compatibility with SY. We confirmed that the system is thermodynamically stable and that device stability, which is one of the important characteristic in applicable LEDs, is also likely to be excellent.

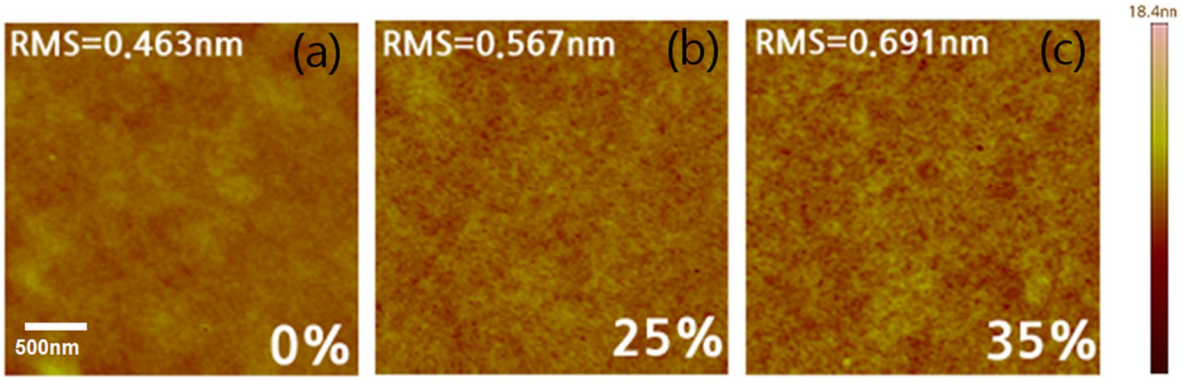

Figure 2.5 AFM images of SY:ILMs blend film with (a) 0, (b) 25, and (c) 35 weight % of ILMs.

The device performances of FTO/ZnO/SY:ILMs blend/Au device with different ILMs content and FTO/SY:ILMs blend (25 wt %)/Au device are presented in Figure 2.6. The device performances were measured using a Keithley 2400 source measurement unit and a (CS-2000) in atmospheric conditions without any encapsulation after initial forward bias of 5.0 V for 30 s for ion redistribution. Compared to the device without any ILMs, those mixed with ILMs in the SY layer showed remarkably enhanced current density. Moreover, the current density of devices using SY:ILMs blends as active layers was enhanced with increasing ILMs content due to the reduced charge injection barriers between each electrode and active layer. The much lower current density for a device using pure SY was attributed to the large energy barriers that bring low device performance. The turn-on voltage of the device made using pure SY was 41.8 V, the maximum luminance was 0.11 cd/m^2 at 44.8 V, and the maximum luminous efficiency was 0.002 cd/A. The devices using SY:ILMs blends showed much

lower turn-on voltages, higher luminance and higher luminous efficiencies.

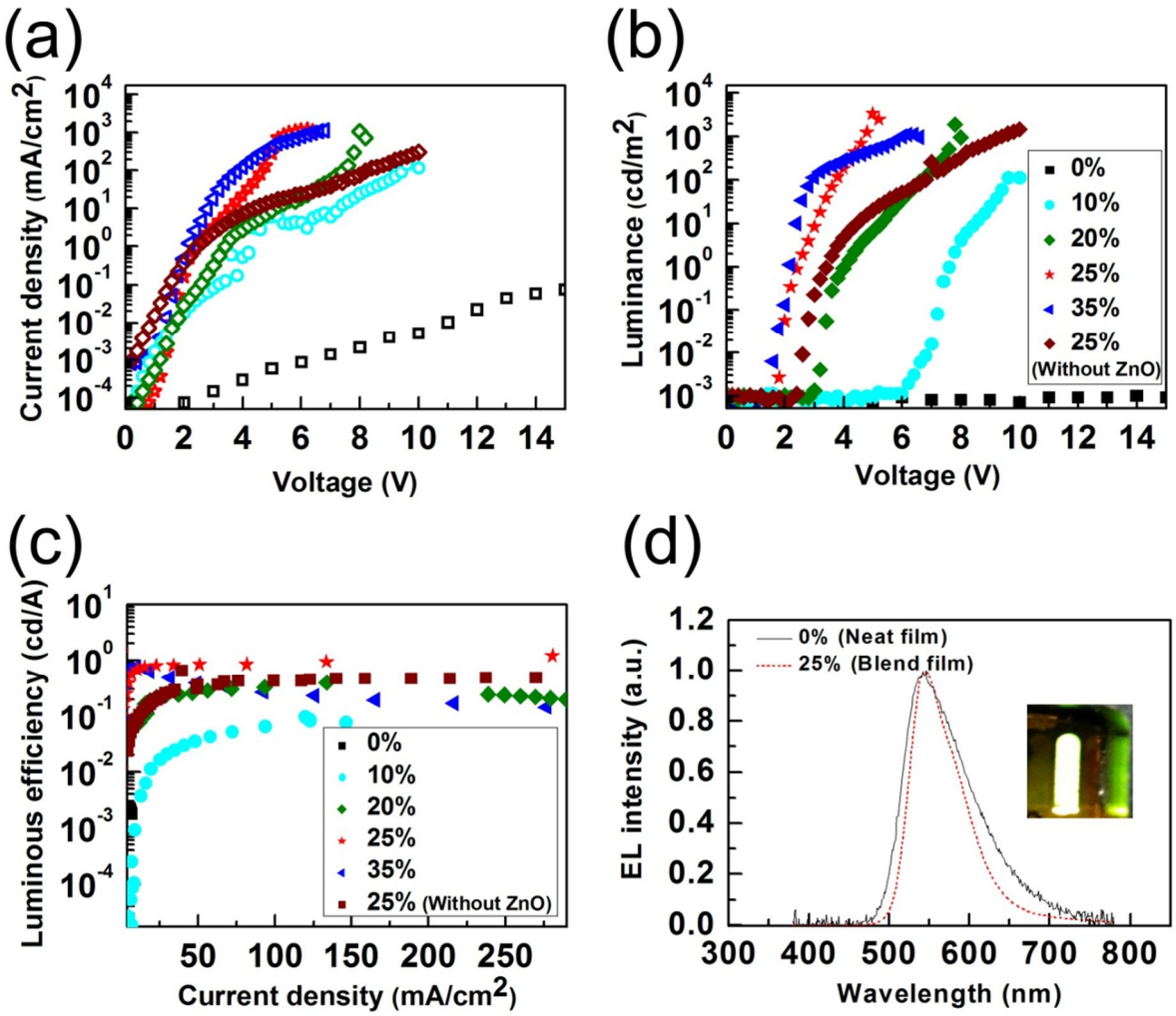

Figure 2.6 Device characteristics of (a) current density vs. applied voltage (*J-V*), (b) luminance vs. applied voltage (*L-V)* and (c) luminous efficiency vs. current density (*LE-J*) curves with SY:ILMs blend films using different ILMs weight percent after initial forward bias of 5.0 V for 30 s for ion redistribution in polymer LECs with and without ZnO layers. (d) Electroluminescence spectra for pure SY and SY:ILMs (25%) blend film.

Table 2.1 Summarized polymer LECs performance of the different ILMs content.

Device Configuration	Turn on (V)	L_{max} (cd/m^2) @ bias	LE_{max} (cd/A) @ bias
FTO / *ZnO* / SY:IL (0 wt.%) / Au	41.8	0.11 @44.8 V	0.002 @42.0V
FTO / *ZnO* / SY:IL (10 wt.%) / Au	7.1	110 @10.0V	0.09 @10.0V
FTO / *ZnO* / SY:IL (20 wt.%) / Au	3.5	1900 @7.8V	0.63 @7.8V
FTO / *ZnO* / SY:IL (25 wt.%) / Au	2.1	3400 @5.0V	1.20 @5.0V
FTO / SY:IL (25 wt.%) / Au (without ZnO layer)	2.9	1500 @10.0	0.65 @7.0V
FTO / *ZnO* / SY:IL (35 wt.%) / Au	1.8	1100 @6.2V	0.74 @2.8V

Table 2.1 summarizes the detailed device characteristics including luminance, luminous efficiency, and turn-on voltage. Although the device performance was improved with increasing ILMs content, there was an optimum condition for the highest luminous efficiency of HyPLECs. Especially, the device with 25 wt % of ILMs in SY and ZnO layer showed the highest device performance with a turn-on voltage of 2.1 V, a luminance of 3400 cd/m^2 at 5.0 V, and a luminous efficiency of 1.2 cd/A at 5.0 V, which correspond to approximately a 600-fold increase compared to the electroluminescence efficiency of pure SY. We also confirmed that the device with ZnO layer showed enhanced device performance (approximately a twofold increase for luminous efficiency) than the polymer LEC without ZnO layer, as shown in Figure 2.6 (a)-(c). Moreover, we measured the luminance and luminous efficiency of polymer LECs with and without the ZnO layer by applying voltage up to 3 V as a function of time in air atmosphere. The luminance and luminous efficiency of polymer LEC without ZnO layer rapidly degrades, whereas the polymer LEC with ZnO layer shows robust air-stability even after 55 h exposure to air, as shown in Figure 2.7. We note that all the devices exhibited original green emission of SY regardless of using the SY:ILMs blend film, as shown in Figure 2.6 (d).

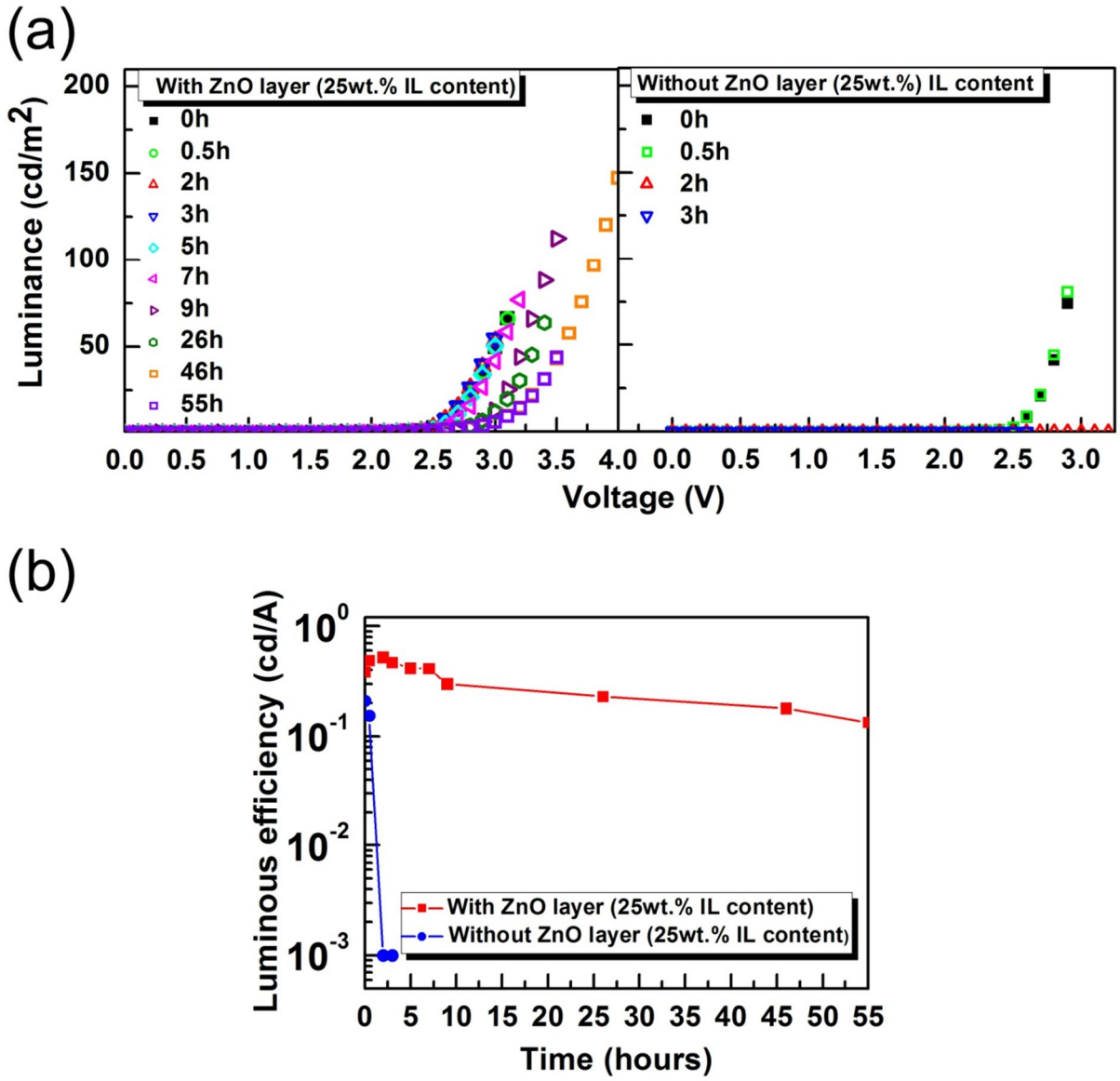

Figure 2.7 (a) Luminance versus voltage (*L–V*) characteristics for polymer LECs with and without the ZnO layer measured as a function of time in air atmosphere. (b) Comparison of the luminous efficiency (*LE*) at 50 cd/m^2 as a function of time for polymer LEDs with and without the ZnO layer.

Figure 2.8 (a) shows the current density-voltage-luminance (*J-V-L*) characteristics of the device under forward and reverse bias. In contrast to the device with the pure SY active layer, electroluminescence of the device with the SY:ILMs (25 wt % of ILMs) blend was also observed under reverse bias (0~18 V). The turn-on voltage is around 3.0 V, which is not quite different from the turn-on voltage in forward bias (0~8 V). Maximum luminance is around 260 cd/m^2 for a reverse bias scan. Figure 2.8 (b) shows the time response of the *J* and *L* under a constant bias of 3.2V in HyPLECs with SY:ILMs (25 wt % of ILMs) blend. It took a few seconds to redistribute the mobile anions near the Au anodes and to redistribute the cations near the transparent FTO/ZnO cathode; charge carriers were injected after

building the electric fields. These results, including high luminance,
high luminous efficiency, low turn-on voltage, the ability to emit light under applied reverse bias, and time response behavior confirmed the LEC behavior in the FTO/ZnO/SY:ILMs blend film/Au structure.

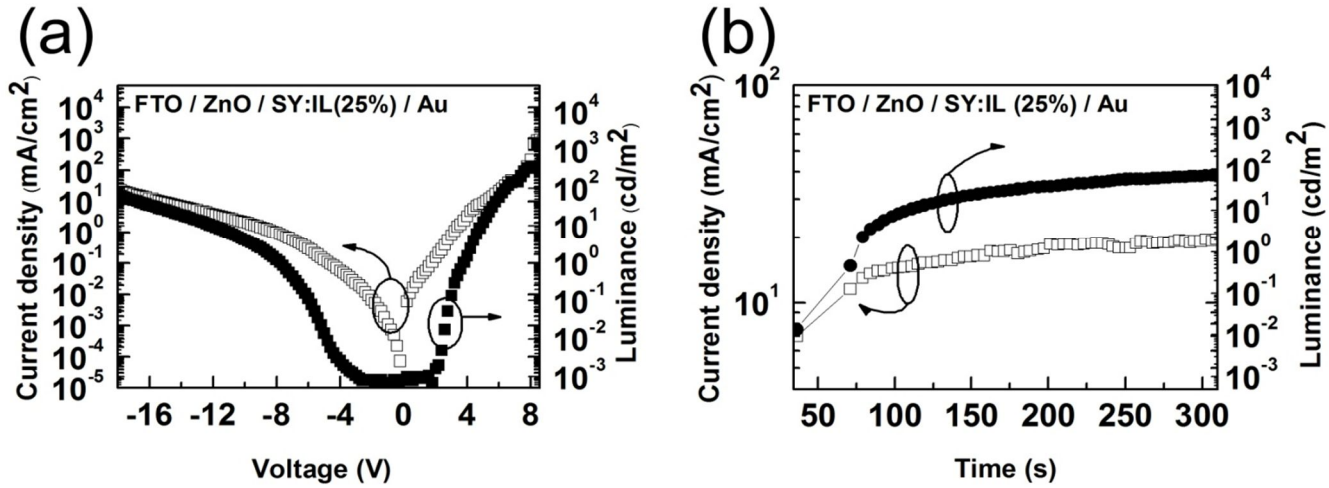

Figure 2.8 (a) Current density-applied voltage-luminance (*J-V-L*) characteristics under forward and reverse bias of the HyPLECs fabricated with SY:ILMs _25%_ blend film. (b) Time response of current density (open symbol) and luminance (closed symbol) for FTO/ZnO/SY:ILMs (25%)/Au configuration under a forward bias of 3.2 V.

2.5 White emission in hybrid organic-inorganic polymer light-emitting diodes (HyPLEC)

2.5.1 Objective and overview of the research

Among various device architectures, hybrid organic-inorganic polymeric light-emitting diodes (HyPLEDs) that utilize metal oxides as charge transporting and injection layers are promising candidates for low-cost, high-performance, and solution-processable flexible displays. One device that exploits this opportunity in an attractive manner is the light-emitting electrochemical cell1s (LECs). In particular, white emission device in hybrid organic-inorganic polymeric light-emitting electrochemical cells (HyPLECs) are cost-effective process since they use white emission fluorescent blend with ionic compound as single active layer in device and solution processable method to deposit a transition metal oxide (TMO) layer. White HyPLECs contains mobile ions in the active material. These ions rearrange during operation, which in turn allows for a range of attractive device properties, including low-voltage operation with thick active layers and stable electrode materials.

2.5.2 Experimental

White PLED exhibits almost the same intensity of blue and orange-red emitting bands which produces a strong white color. 1) Preparation of white emitting light-emitting polymer (LEP) blend solution: As a host polymer, we used soluble poly-spiro-bifluorene copolymer (purchased from Merck, SPB-02T). It shall be referred to as “M-blue” in this study. DCM dye is doped to M-blue host matrixand the doping concentration of DCM was selected with 1.0% and 0.5% by weight. The HyPLECs were prepared by the sequential deposition of fluorine doped tin oxide (FTO), ZnO, M-blue:DCM:IL active layer, and Au layers. An 80 nm thick n-type ZnO layer was prepared by spray pyrolysis deposition from 80 mg mL^{-1} zinc acetate dihydrate/methanol precursor solutions. A 100 nm thick white emission blend as emissive layer was spin cast from 11 mg mL^{-1} toluene solutions onto the ZnO surface, and then thermal annealing was performed at 85 °C for 1 h under a nitrogen atmosphere. A 10 nm thick MoO_3 layer and a 70 nm thick Au layer were subsequently evaporated on the active layer to complete the device fabrication.

2.5.3 Results and discussion

Figure 2.9 illustrates the device architecture of inverted type PLEDs used in this work. By mixing M-blue as a host and DCM as orange emitter dye, we could obtain the white light in a single layer and ionic liquid material (Aldrich) as an ion supply was added to the blend solution at the same time to

achieve the LEC characteristics. As a transparent cathode, ZnO layer also serve as electron injection layer and hole blocking layer.

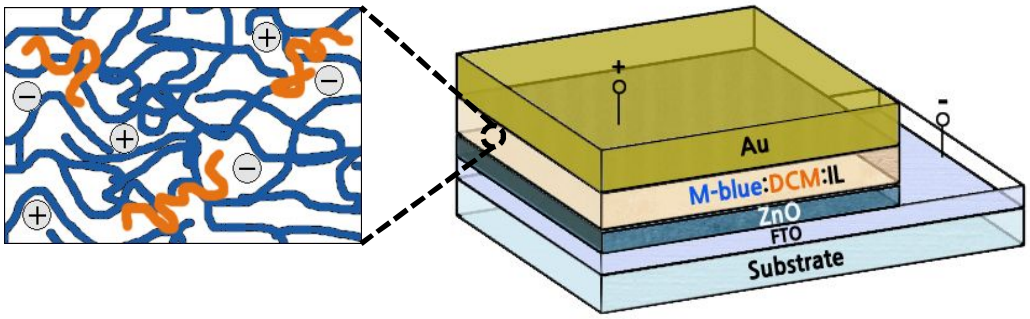

Figure 2.9 Schematic representation of the white-radiating device with HyPLEC architecture.

The UV-absorption and photoluminescence (PL) characteristics of the host "M-blue" and orange-emitter dye are shown in Figure 2.10. The neat M-blue film exhibits PL emission peak at 460 and 490nm. Absorption peak of DCM was 475nm.

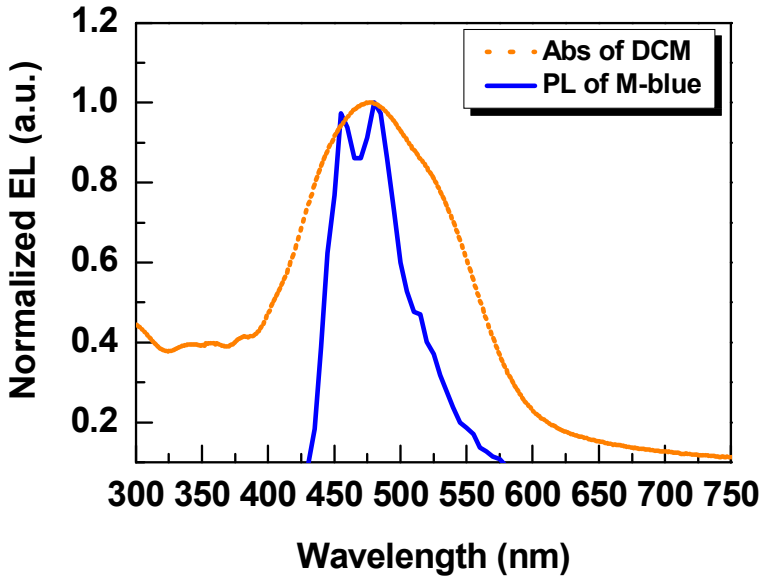

Figure 2.10 Normalized UV-vis absorption (dashed line) of DCM and photoluminescence (PL) (solid line) spectra of M-blue in the neat film.

White emission was obtained in virtue of the balanced intensity of the blue and orange emission peak in EL spectra by weight percentage of 0.5% of DCM dye as displayed in Figure 2.11. The CIE

diagram is also shown in Figure 2.12. The CIE color coordinates are (0.4199, 0.3917) and (0.3234, 0.3209) for doping concentrations of 1.0wt% and 0.5wt%, respectively. As a consequence, we have successfully obtained pure white emission of (0.3234, 0.3209), corresponding to near the white emission of (0.33, 0.33).

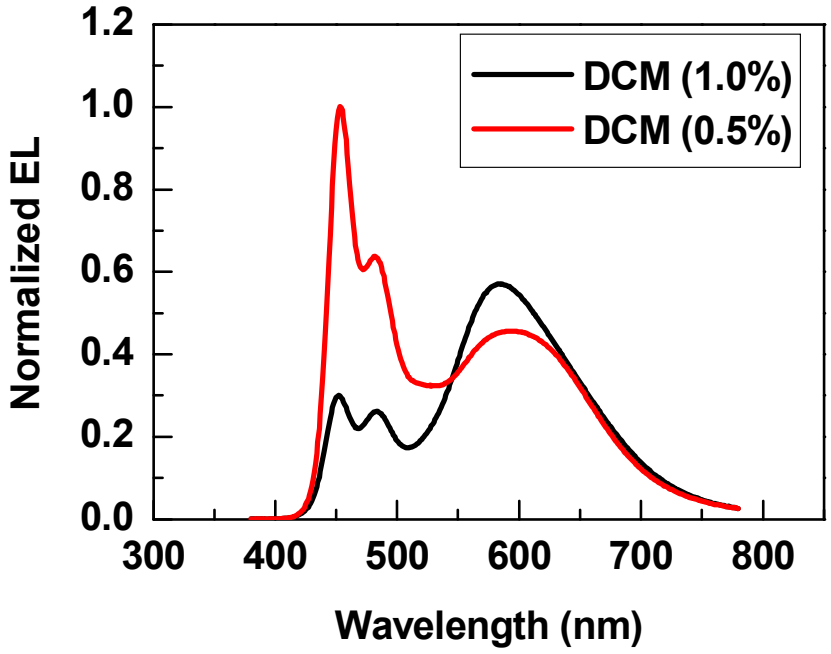

Figure 2.11 Normalized EL intensity with different concentration of the DCM dye. It shows the color stability of FTO/ZnO/M-blue:DCM:IML/Au.

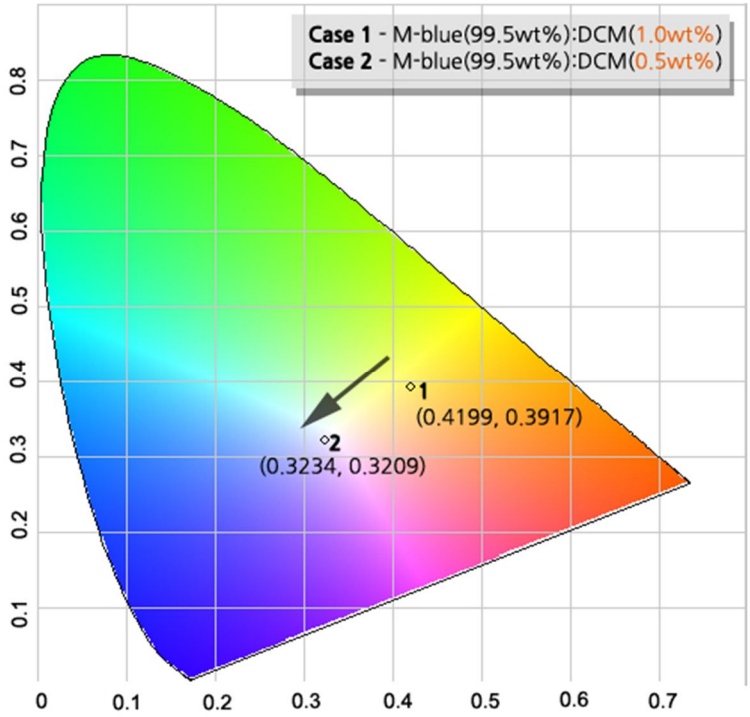

Figure 2.12 CIE diagram with different composition of the dopant. It shows the color stability of FTO/ZnO/M-blue:DCM:IML/Au.

Figure 2.13 (a), (b) assemble the device characteristics of a HyWPLEC. Maximum luminance value of 3700 cd/m^2 is reached at 11.0V and the EL turn-on voltage is observed at 2.2V. The luminous efficiency peaks at 0.79 cd/A around 4000 cd/m^2.

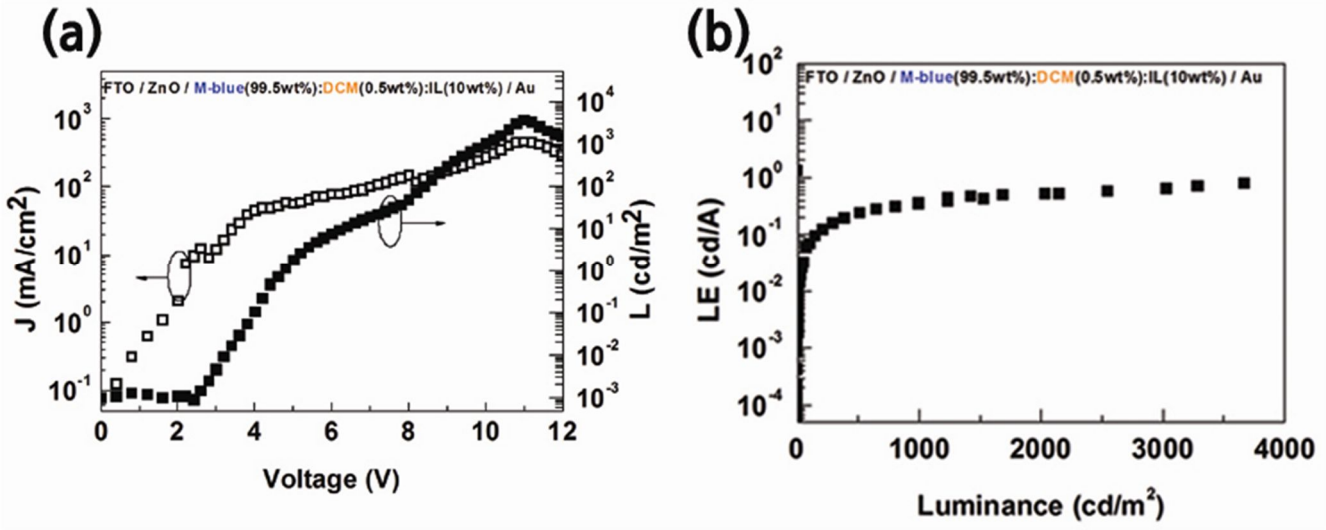

Figure 2.13 (a) Current density (J) - Voltage (V) – Luminance (L) characteristics and (b) luminous efficiency (LE) as function of current density (J) for the four devices.

Chapter 3 Ternary fluorescent polymer blend: White polymer light emitting diodes (WPLEDs)

3.1 Objective and overview of the research

White polymer light-emitting diodes (WPLEDs) have attracted significant research attention because they can be combined with RGB color filters to create full-color displays.[60] In particular, white light emission devices with polarized emission will make it possible to use in potential application such as high-contrast displays, efficient power-saving backlight sources, optical data storage and optical communication.[61] Possibly the most straightforward way to generate white light is to blend emitting polymers into a single layer. In this study, our WPLEDs were prepared by mixing the primary red, green, and blue (RGB) emitting polymer (LEP). Ternary blending method is the most attractive method to realize white emission EL device because of facile film formation, large scale production possibilities, and cost effective features in technical aspects. Polymer blends also show low turn on voltage, high brightness, high efficiency, and color purity in WPLEDs. After fabrication of WPLEDs, we attached the right-handed cholesteric liquid crystal (R-CLC) reflector to obtain circularly polarized white light emission. By attaching a R-CLC reflector to an WPLED device, we observed LCP- white emission due to the selective reflection of the CLC film.

3.2 Research background

There are several methods to prepare the white light-emitting diodes (WLEDs) based on organic materials. One of the approaches to produce a white emission is to use a multilayer structure consisting of the primary colors.[62-64] However, multilayer devices are difficult to fabricate by solution processing, because it is very hard to find a solvent that selectively dissolves the material being deposited without dissolving the previously deposited underlayers.[65,66] Thus, several methods have been reported for realizing WPLED with a polymer blends, including single emitting polymer layer doped with fluorescent dyes,[67-73] and a phosphorscent Ir-complex[64,74-76] and a single polymer with an emitter moiety in the polymer main chain.[77,78]

We focus on the polymer blended single layer system in WPLEDs. The WPLEDs can be fabricated by mixing the RGB light-emitting polymers. To realize white light emission, the manipulation of composition of RGB light-emitting polymers (LEPs) is necessary. White emission shows broad range of spectrum with Commission Internationale de L'Eclairage (CIE) coordinates (x , y) of (0.33 , 0.33). In blends of emitting dyes and host, they require a precise control of doping level in order to suppress the complete Forster energy transfer between the components.

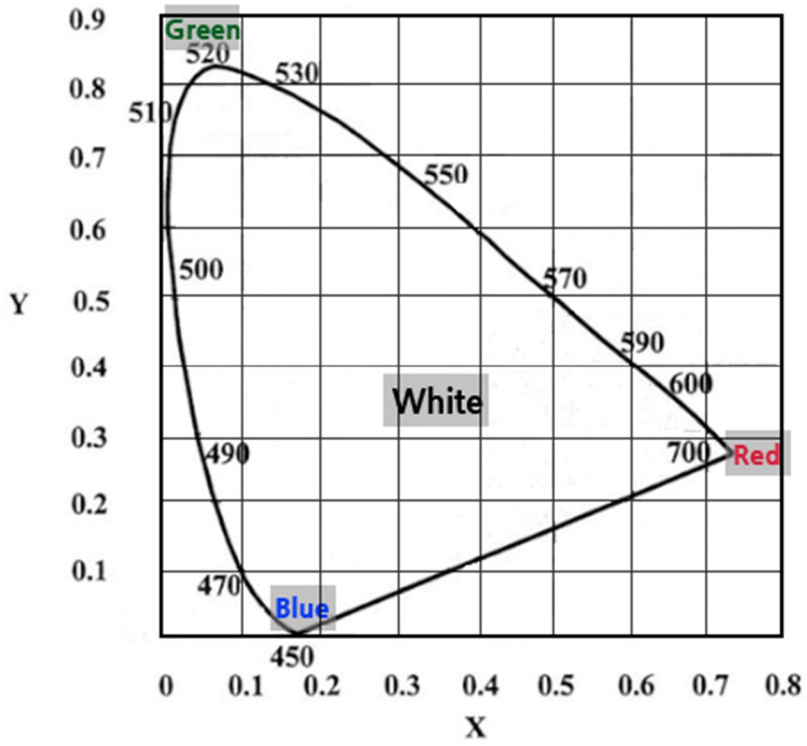

Figure 3.1 CIE 1931 chromaticity diagram with distinct colors.

In order to show the spectrum properties of WPLED, CIE coordinate is helpful in visualizing the

emission color as depicted in Figure 3.1. It is based on the peculiarities of the three types of cones in the human eyes, which are sensitive of each blue, green, or red radiation. The corresponding wavelength marks the corners of the chromaticity diagram. When the spectral width of the light increases and the emission is therefore less pure, the color coordinates move towards the center. For example, "white light", that is, the broad emission spectrum of a black-body radiator heated to very high temperatures (e.g., the sun), is described by a point in this diagram at which x as well as y are about 33%.

The compatibility of ternary fluorescent polymer blends results in significant blue emission band change with green and red incorporated into blue host matrix. Most polymers are not miscible with each other because of their low value of entropy of mixing .[79] It brings about phase separation, which can cause several problems, such as the variation of the color with the applied voltage and low efficiency. Making a homogeneous polymer blends is very important to enhance the device performances and the miscibility can be improved by blending the copolymers that have same moiety.[80,81]

3.2.1 Forster and Dexter energy transfer

Energy transfer occurs between two molecules which are called intermolecular process. A molecule in an excited electronic state, which is called a 'donor', may transfer its energy to another molecule, which is called an 'acceptor'. After this process, the donor molecule returns to its ground electronic state and the acceptor molecule is promoted to higher state, which can be represented as

$$D^* + A \rightarrow D + A^*, \tag{3.1}$$

Where D and A are the donor and acceptor. The asterisk denotes the excited state. Energy transfer can be a two-step process without direct interaction between the donor and acceptor molecules as follows:

$$\begin{aligned} D^* &\rightarrow D + hv, \\ hv + A &\rightarrow A^* \end{aligned} \tag{3.2}$$

Here, photons from the radiative recombination of donor are absorbed by the acceptor and promote the acceptor to an excited state. This is called radiative energy transfer since photons are involved in this process. The strength of this energy transfer only depends on the emission efficiency of the donor and the absorption efficiency of the acceptor at this wavelength. A single process without the intermediation of photons, described by Equation 3.1, is also possible when donor and acceptor molecules are close (less than 10nm), which is called nonradiative energy transfer, through the energetic resonance of two molecules. As shown in Figure 3.2, this process is transfer probability is proportional to the spectral overlap (J) between donor emission ($I_D(v)$) and acceptor absorption ($\varepsilon_A(v)$) spectra, as follows:

$$J = \int_0^\infty I_D(v)\varepsilon_A(v)dv \tag{3.3}$$

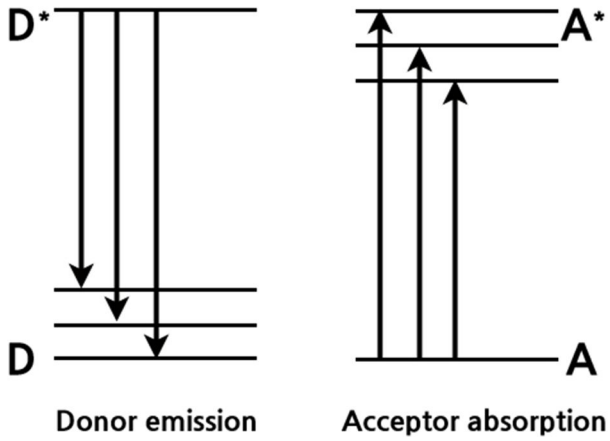

Figure 3.2 Electronic energy level representations for donor emission and acceptor absorption.

Among a number of energy transfer mechanisms, Förster and Dexter energy transfer are two well-known types of transfer. Förster energy transfer, also called Förster resonance energy transfer, describes an energy transfer mechanism between two fluorescent molecules as shown in Figure 3.3. A fluorescent donor molecule is excited at its specific fluorescence excitation wavelength. By a long-range dipole-dipole coupling mechanism, this excited state is then nonradiatively transferred to a second molecule, the acceptor. The donor returns to the electronic ground state. When both molecules are fluorescent, the term fluorescence resonance energy transfer (FRET) is also used, although the energy is not actually transferred by fluorescence. The FRET efficiency is determined by three parameters: 1) Distance between the donor and the acceptor. 2) Spectral overlap of the donor emission spectrum and the acceptor absorption spectrum 3) Relative orientation of the donor emission dipole moment and the acceptor absorption dipole moment. Due to the fact that the donor exciton relaxation energy is typically smaller than the absorbed photon energy (e.g., due to Stokes shift), the Förster energy transfer would result in gradual energy reduction of spectra red-shift along the exciton diffusion or propagation direction. The most efficient Förster energy transfer occurs when the acceptor energy gap matches the donor emitted photon energy well, i.e., transfer coupling may be poor if the acceptor gap is too far away compared to the donor exciton energy. Also, the Förster energy transfer can occur between two remote sites above 10nm and is sensitive to molecular dipole orientation.

In contrast, in a Dexter energy transfer process as shown in Figure 3.4, the electron near D-LUMO first transfer to the A-LUMO, and the hole near the A-HOMO at the same time transfers to L-HOMO, the electron at A-HOMO then relaxes with the hole at A-HOMO to form a new exciton, so it may be regarded as two separate charge transfer processes occurring simultaneously. Because of this, Dexter energy transfer can only proceed at close or adjacent sites (typically <1nm), and it can proceed with both singlet and triplet exciton transfer, while Förster energy transfer can only proceed with singlet exciton transfer. Moreover, the A-HOMO and A-LUMO both are desirably located within the

energy gap of the D-HOMO and D-LUMO in the Dexter energy transfer (Figure 3.4), while the relative positions of HOMO and LUMO are not crucial in Förster energy transfer as long as the energy gap of the acceptor matches the donor excition emission. Even if the gap of the acceptor does not match the donor exciton emission well, Dexter energy transfer may occur as long as the energy offsets between the donor and acceptor are optimal for charge transfer.

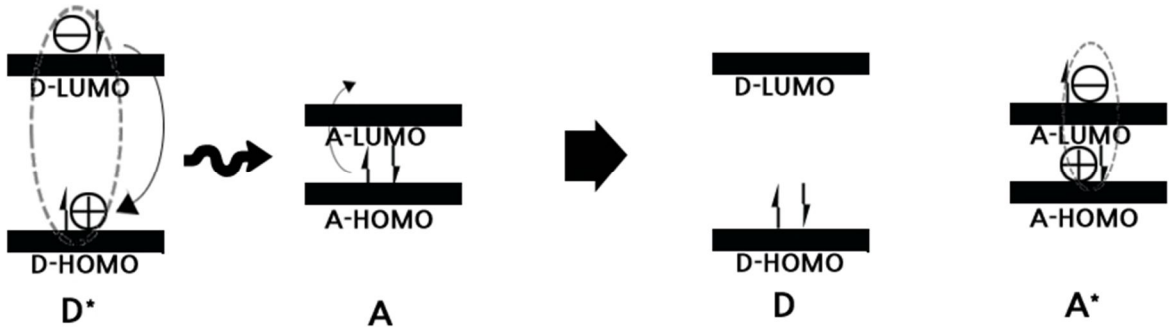

Figure 3.3 Scheme of Förster energy transfer.

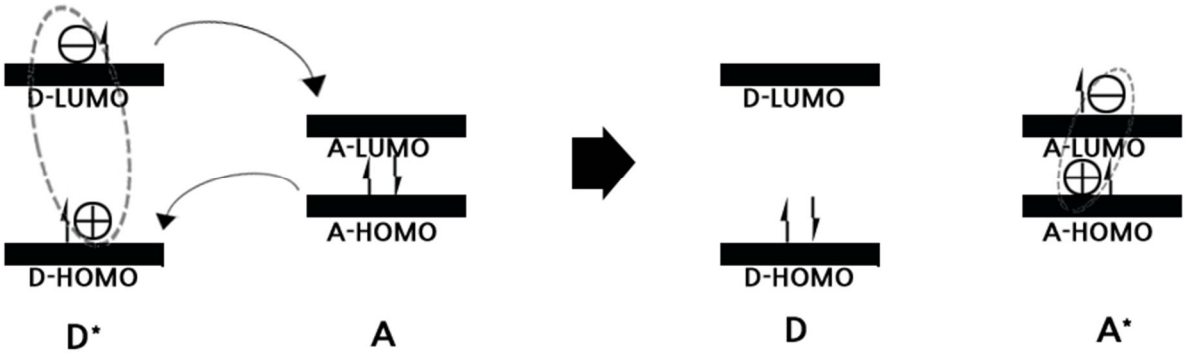

Figure 3.4 Scheme of Dexter energy transfer mechanism

3.2.2 Energy transfer in the polymer blend

The dipole-dipole interaction between two molecules induces a Förster-type non-radiative energy transfer of the excitation energy from a donor to an acceptor. By dispersing small amount of a fluorescent dye into host matrix, it can lead to significant changes in the color of luminescence and an improvement in the device efficiency. However, this simple mixing of ternary fluorescent polymer is difficult to control color balancing. Even though amount of dopant is very small, the emission is dominant from lower band-gap dopants.[65,67,82] This inherent problem arises from the Förster-type energy transfer, which occur in a cascade manner, between the higher band-gap donor and the closely located lower band-gap acceptor by means of spectral matching.[83] The exciton diffusion between host and dopant may take place via the Forster energy transfer.[84] This is a dipole-dipole mechanism whose efficiency depends on the overlap between the donor emission spectrum and acceptor absorption spectrum. The rate constant (k_{ET}) of the Förster energy transfer can be represented as

$$k_{ET} \approx \frac{f_D f_A}{R_{DA}^6 v^2} J \tag{3.4}$$

where f_D and f_A are the transition probabilities for donor emission and acceptor absorption, following the Frank-Condon principle, and R_{DA} is the distance between donor and acceptor molecules. The Förster radius, R_{DA} is considered as a measure of the energy transfer efficiency between donors and acceptors. Since Förster theory is based on individual interaction of donor and acceptor molecules, concentration of either donor or acceptor is not considered in calculating the Förster radius. Therefore, it may not be an accurate way to estimate the energy transfer efficiency only from the Förster radius in the system with varying donor/acceptor concentrations such as polymer blend films.[85] Energy transfer will take place between donor and acceptor when the spacing between uniformly mixed donor and acceptor polymers is on the order of tens of Augstroms. Moreover, the energy transfer rate between donor and acceptor should be faster than any decay rate of excited states in donor polymer. We expect that its EL spectra will be composed of host and dopant light emission in polymer blend system. Energy transfer competes with both radiative and nonradiative decay inside the donor polymer. It is also expected that a diluted material in a host matrix can produce enhanced light emission intensity[86] since increasing the interchain separation between the polymer chains by diluting the polymer in a solid-state matrix can reduce the non-radiative transitions as observed in solution. [87] Moreover, it is expected that optimized blend PLED could produce much higher luminance and luminous efficiency than single polymers.

3.2.3 Cholesteric liquid crystals (CLCs)

Circularly polarized white light can be produced by using WPLEDs combined with a wide-band width cholesteric liquid crystal (CLC) reflector. CLC materials are special types of quarter-wave stack reflectors in which refractive index, in a periodic helical structure with a pitch length (P), continuously varies from n_e to n_o which are extraordinary and ordinary refractive indices of the liquid crystal. The CLC reflector is depicted in figure 3.5.

A CLC is formed by rod-shaped molecules that arrange themselves within a helical structure. In planes perpendicular to the helical axis, the molecules show a nematic-like order, and the preferred direction of molecules defining the local optical axis, director. Along the helical axis, the director is continuously rotated in successive layer to form a periodic helical structure with a period pitch $P = 2a$ which can be either right or left-handed. In a certain frequency range, a CLC shows selective reflection of that mode for which the polarization has the same handedness as the cholesteric medium[88,89] In selective reflection in CLCs, it is well known that circularly polarized light is totally reflected when it is incident along the helical axis of the CLC phase, and the wavelength and helical handedness are the same as those of the CLC. It means that light having the same handedness of the CLC helix cannot propagate with a frequency range within the stop band[88,89] The RCP light with the opposite handedness to the L-H photonic band gap (PBG) helix is transmitted through the first L-H PBG layer, but then changes its polarization state to the opposite circular polarization (LCP), which is selectively reflected by the second L-H PBG layer. This reflection directs the light back through $\lambda/2$ plate defect layer, wherein the polarization again returns back to RCP, to give higher reflection over 50% as depicted in Figure 3.6.

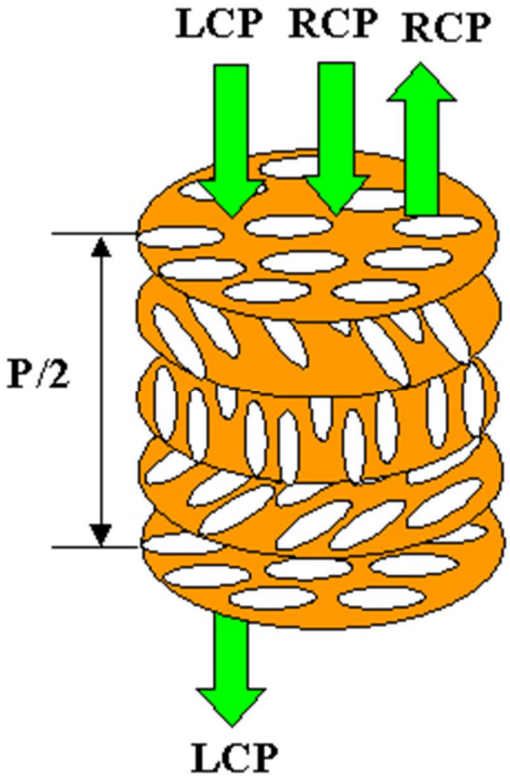

Figure 3.5 Selection rule for the reflection and transmission of light by CLC.

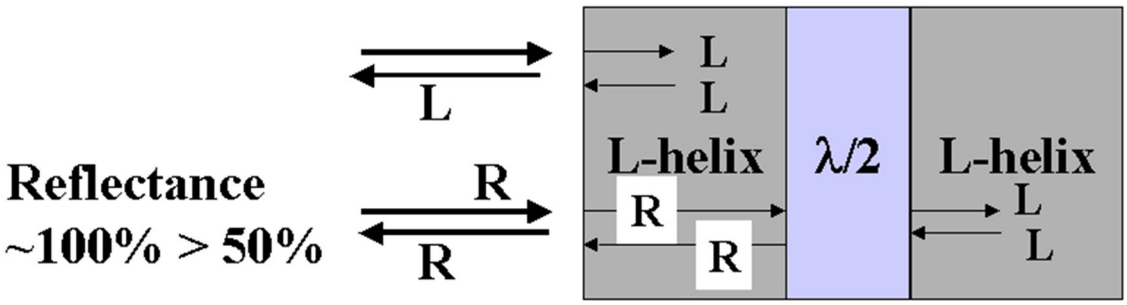

Figure 3.6 Mechanism of higher reflection of Plusiotis resplendens.

3.2.4 Unpolarized white light into circularly polarized light

In an OLED, a substantial fraction of the emitted light does not escape directly, but only escaped following reflection from the metal cathode. This reflection reverses the sense of circular polarization.[90] A first approach to highly circular polarized emission was pioneered by Pollmann et al. [91] in 1976, based on the immersion of fluorescent dyes into a CLC host. Recently, Chen et al.extended this work into the "resonance" regime, where the emission matches the reflection wavelength ("PBG") of the CLC host. [92] An alternative approach to circularly polarized emission is to attach chiral side chains to a fluorescent conjugated polymer as first demonstrated by Langeveld-Voss.[93] Using this approach, circular polarized-electroluminescence (CP-EL) could be demonstrated for the first time.[94]

Belayev et al. have developed a "photon recycling" scheme that exploits the unique properties of CLC chiroselective reflectors[95] Unpolarized light is represented as an equal intensity superposition of left- and right- handed light. The CLC reflector reflects only CP light with matching chirality, but without changing its handness. The metal mirror conversely reflects light of both circular polarizations, but always with a change of handedness. It thus "recycles" photons that were unable to exit through the CLC reflector on their first approach. If the recycling process is ideal then all of the light will escape and will be CP with a sense of chirality opposite to the handedness of the CLC.

The degree of circular polarization is quantified by the wavelength-dependent g-factor :

$$g(\lambda) = 2\frac{r(\lambda) - 1}{r(\lambda) + 1} \tag{3.5}$$

where $r = I_l / I_r$ is the intensity ratio between left- and right- handed CP light. By definition, $-2 \leq g \leq 2$; g = 0 corresponds to non-CP light.

3.3 Experimental

Preparation of white emission LEP blend solution : As a host polymer, we used soluble poly-spiro-bifluorene copolymer (purchased from Merck, product number is SPB-02T). It shall be referred to as "M-blue" in this study. Soluble poly(*p*-phenylene vinylene) (PPV) copolymer known as "Super Yellow" (purchased from Merck) was used as a fluorescent green-emitting dopant and soluble poly-spiro-bifluorene copolymer (purchased from Merck, product number is SPR-001) which is also referred to as "M-red" was also used as a fluorescent red-emitting dopant. Detailed chemical structures are shown in Figure 3.7 (a)-(b). All three fluorescent polymers are dissolved in toluene (11mg/ml) and the concentration of the dopants was controlled by adding the appropriate amount of a diluted toluene solution of the SY and M-red dopants. At first, the concentration of SY was determined by adding the different amount of SY in M-blue matrix. Then, doping concentration of M-red was varied from 0 to 0.5wt% in M-blue matrix with optimized composition (0.075 wt%) of SY.

The procedure of device fabrication procedure ; Glass substrates with patterned indium-tin-oxide (ITO) with a sheet resistance of 20 Ω per square were carefully cleaned with detergent followed by treatment in ultrasonic bath using in succession with DI water, acetone and IPA for 10min, respectively. The substrates were dried in vacuum oven and treated with UV/Ozone cleaner for 20 min. A thin film of Poly(3,4-ethylenedioxythiophene) doped with polystyrene sulphonated acid (PEDOT:PSS) (Clevios P VP Al 4083 supplied by H.C. Starck) was spin-coated onto the ITO-patterned glass at a speed of 4000 rpm and baked at 140 °C for 10min. Ternary blend solutions as emitting polymers were successively deposited onto the PEDOT:PSS layer at a speed of 2000 rpm to give a 100-nm thick. Thermal annealing was performed at 150℃ for 1 hour in a glove box. The LiF(1nm)/Al(100nm) cathodes were deposited by thermal evaporation under high vaccum (< 10^{-6} Torr).

Absorption spectra were obtained with Cary 5000 UV-Vis spectrophotometer (Varian, USA) and photoluminescence (PL) spectra were recorded using FLS920 spectrophotometer (Edinburgh instrument Ltd.) equipped with a 150W xenon lamp at room temperature.

The current density (J) - voltage (V) - luminance (L) characteristics of the devices were measured with a computer controlled Keithley 2400 source meter. A chroma Meter CS-2000 (Konica Minolta Sensing, INC.) was used to detect the electroluminescence (EL) of the devices.

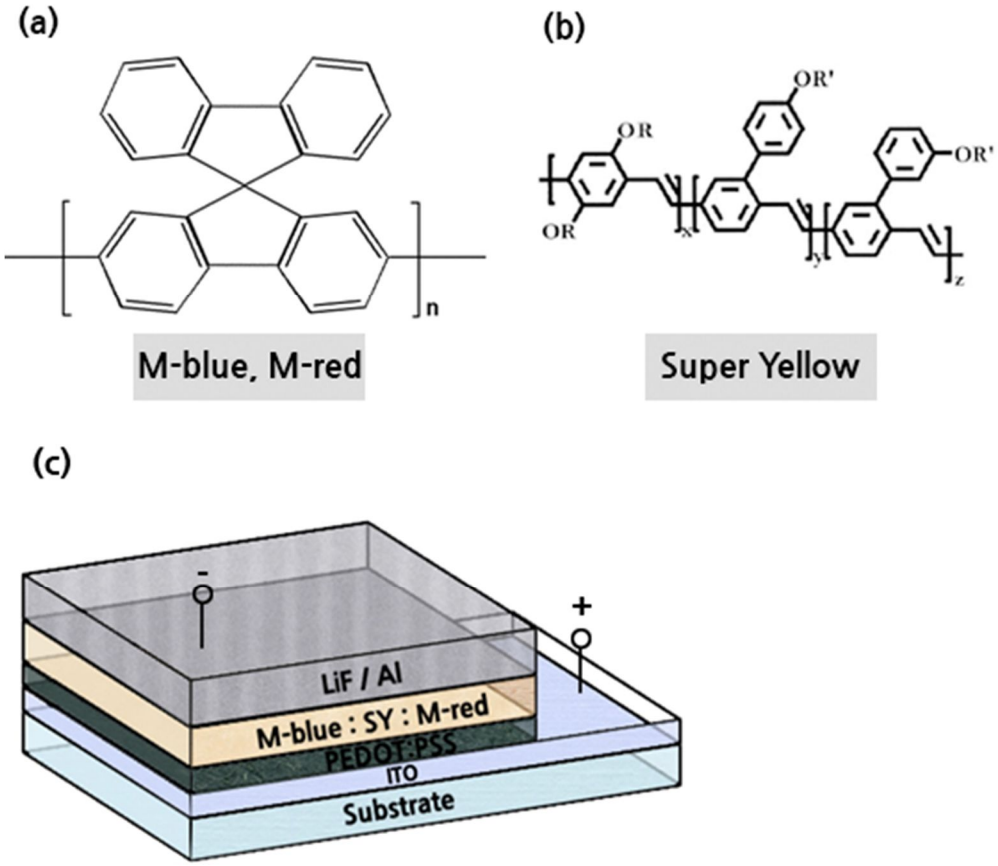

Figure 3.7 (a) Chemical structures of poly-spiro-bifluorene copolymer and (b) PPV copolymer (SY). (c) Device configurations used in this study. The device was constructed as ITO/PEDOT:PSS/M-blue:SY:M-red/LiF/Al.

3.4 Results and discussion

The UV-absorption and photoluminescence (PL) characteristics of the host and dopant fluorescent polymers are shown in Figure 3.8. The neat M-blue film exhibits UV absorption peak at 380 nm and PL emission with peaks at 460 and 490nm. SY shows absorption peak at 390 nm and PL emission peak at 550nm. M-red shows the absorption peak with intense peak at 330 and PL emission peak at 640nm.

In principle, the energy transfer from the host (M-blue) to acceptor (SY) should occur because the PL spectrum of M-blue overlaps well with absorption spectrum of SY. Spectral overlap, therefore, meets the necessary condition of Förster energy transfer. However, the energy transfer efficiency is very sensitive to the distance between the donor and acceptor. Thus, white emissions were obtained by partial energy transfer from dilution of the SY and M-red polymer concentration in M-blue polymer.

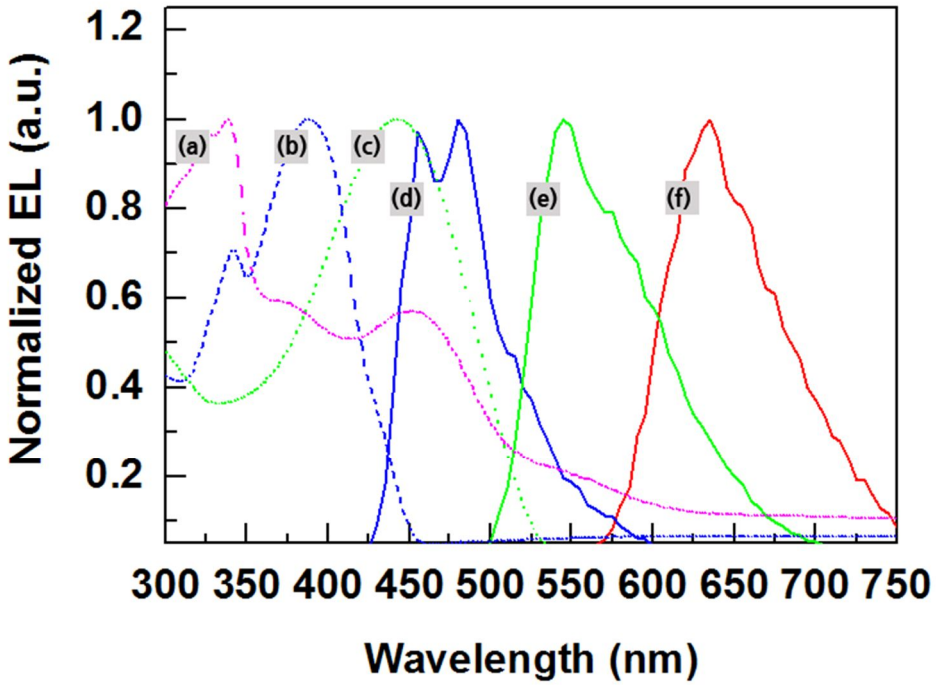

Figure 3.8 Normalized UV-vis absorption (dashed line) and photoluminescence (PL) (solid line) spectra of M-blue, SY and M-red in the film (a) absorption of the M-red film, (b) absorption of the M-blue film, (c) absorption of the SY film, (d) PL of the the M-blue film, (e)PL of the SY film, (f) PL of the M-red film.

Normalized EL spectra of a series of devices with different concentration of dye into the M-blue host

are presented in Figure 3.9. The amount of green-emitting fluorescent dye, SY incorporated into M-blue matrix is pre-conditioned with composition of M-blue:SY = 99.4:0.075 by weight. EL spectra are very sensitive to polymer blend composition. Therefore, a slight change in red-emitting dye from 0.5wt% to 0.3wt% could result in the prominent red or blue light-emission, respectively. At a concentration of 0.3wt%, the spectra moved to blue emission region because carrier trapping can occur in low-gap dopant polymer. The device with composition of M-blue : SY : M-red = 99.4 : 0.0075 : 0.5 blend ratio by weight exhibited white emission characteristic due to the increase of M-red peak intensity. This device showed EL spectra covering the whole visible range from 400 to 750 nm and exhibited three balanced emission peaks located at the RGB three primary colors. The EL intensity of the green emission peaks was equal to the blue emission peak for optimized white emission blend device, even though the amount of SY (0.075wt%) was small in M-blue (99.4wt%) matrix. This implied that Förster type energy transfer occurred from M-blue to SY. When the concentration of the M-red was decreased, the red fluorescence was reduced and the blue fluorescent component with the typical features of M-blue emission started to rise.

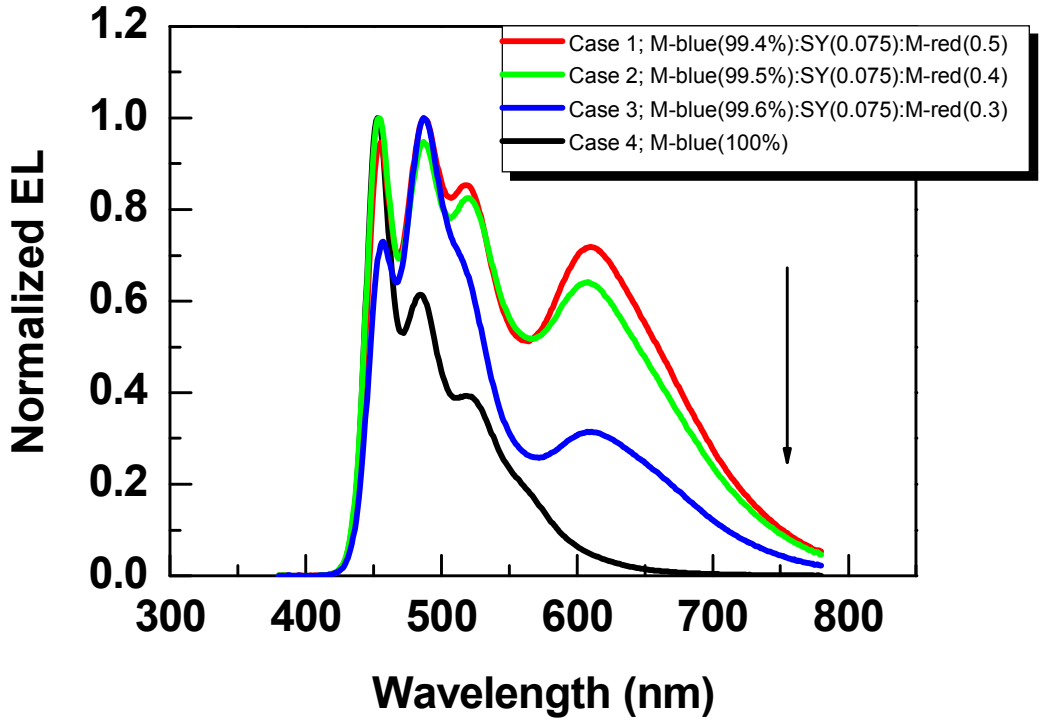

Figure 3.9 Normalized EL spectra of white emission in PLEDs with varying the composition of red polymer dopant.

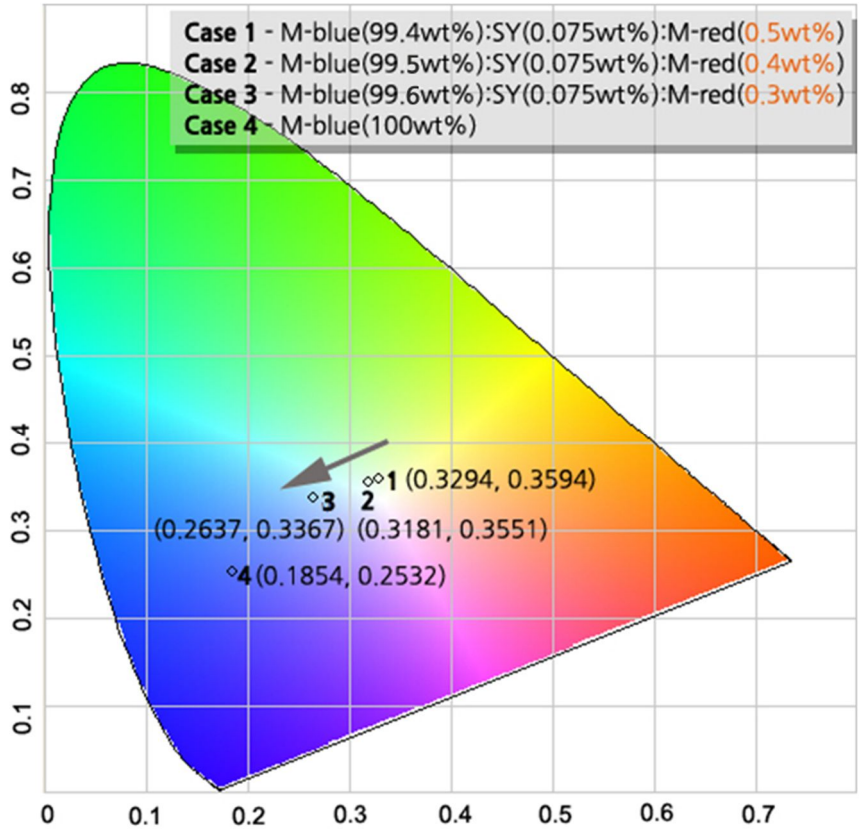

Figure 3.10 CIE color diagram of white emission in PLEDs with varying the composition of red polymer dopant.

This behavior can be observed through the 1931 Commission Internationale de L'Eclairage CIE coordinates as shown in Figure 3.10. The color coordinates dramatically move with only small changes in the amount of M-red doping in the M-blue matrix. At a concentration of 0.5wt% of M-red doped into M-red host, the CIE coordinates are (0.33, 0.36) corresponding to whitish emission.

Figure 3.11 shows the EL spectra of the white emission device with M-blue(99.4wt%)/SY(0.075wt%):M-red(0.5wt%) ternary blend measured at varying applied voltages. The white EL spectra slightly changed with different voltages or different luminace. The CIE color coordinates of white PLEDs under different driving voltages are shown in Figure 3.12. For the device, the CIE coordinates were very close to pure white color coordinates, and remained very stable at a relatively wide bias. The CIE coordinates of the luminescence changed from (x=0.349, y=0.3597) at 7.0V to (x=0.3081, y=0.3335) at 13.6V.

The measured luminance, current density, luminous efficiency and CIE coordinates are presented with applied voltage to the device in Table 3.1.

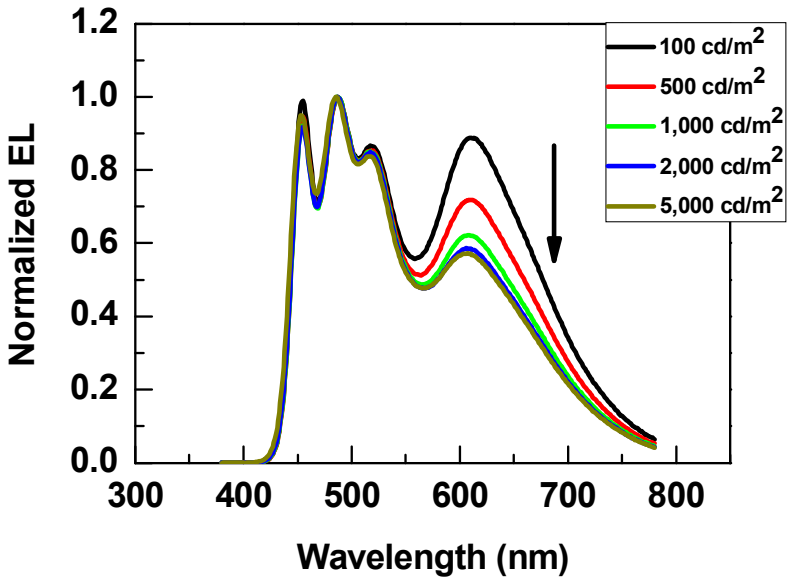

Figure 3.11 Color stability of white emission PLED with composition of M-blue:SY(0.075wt%):M-red (0.5wt%)

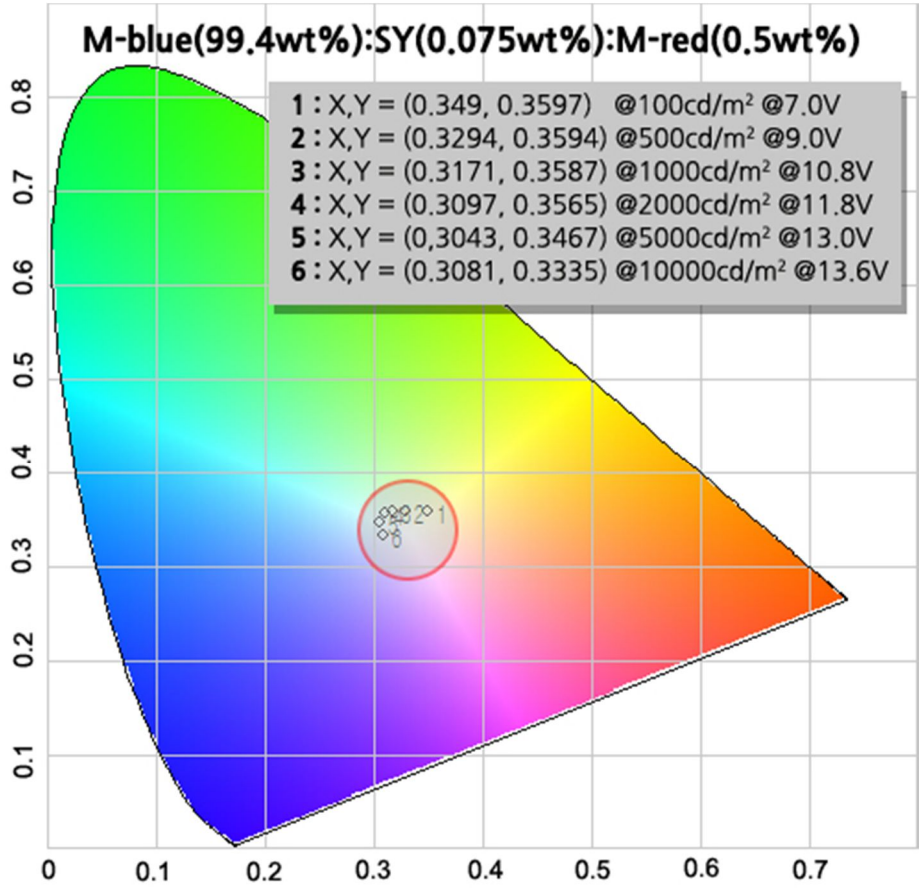

Figure 3.12 Color stability of PLED with composition of M-blue(99.4wt%):SY(0.075wt%):M-red (0.5wt%).

Table 3.1 Detailed device characteristics of PLEDs with various composition of red dopant.

Voltage (V)	Luminance (cd/m^2)	Current density (mA/cm^2)	Current efficiency (cd/A)	CIE coordinates (X,Y)
7.0	100	2.9	3.78	(0.3490, 0.3597)
9.0	500	9.5	4.52	(0.3294, 0.3594)
10.8	1000	23.6	4.67	(0.3171, 0.3587)
11.8	2000	46.8	4.62	(0.3097, 0.3565)
13.0	5000	125.5	4.24	(0.3043, 0.3467)
13.6	10000	284.8	3.39	(0.3081, 0.3335)

Figure 3.13 and 3.14 show the electrical characteristics of a PLED made with a 99.4 : 0.075 : 0.5 blend ratio by weight. The J-V-L characteristics of the devices fabricated from white polymer blend revealed that the turn-on voltage was 2.4V, the maximum luminance was 10000cd/m^2 at 13.6V, and the maximum luminescence efficiency of the polymer LEDs with white polymer blend was 4.67cd/A at 10.8V.

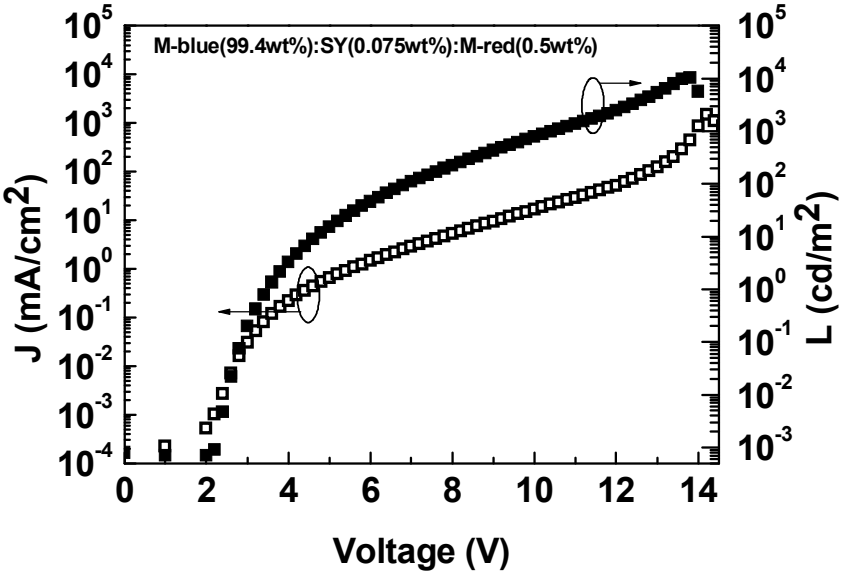

Figure 3.13 Current density (J) and luminance (L) versus applied voltage (V) for white emission device of ITO/PEDOT:PSS/M-blue(99.4wt%):SY(0.075wt%):M-red(0.5wt%)/LiF/Al configuration.

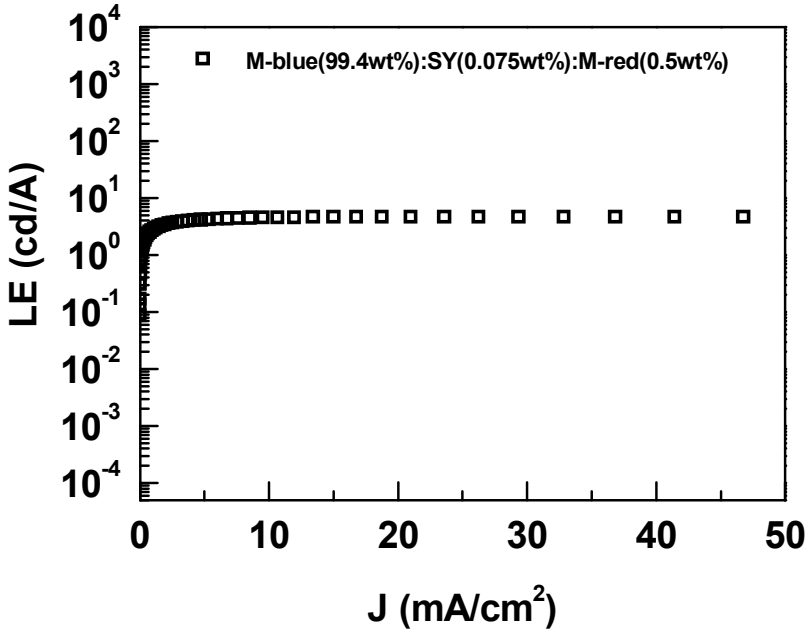

Figure 3.14 Luminous efficiency (LE) versus current density (J) for white emission device of ITO/PEDOT:PSS/M-blue(99.4wt%):SY(0.075wt%):M-red(0.5wt%)/LiF/Al configuration.

After the WPLEDs were ready, we attached the right-handed cholesteric liquid crystal (RH-CLC) reflector to obtain circularly polarized white light emission. The device configuration is depicted in Figure 3.15 (a). The emission from WPLEDs passes through or is refected from the RH-CLC reflector due to the selective reflection of the CLC film. The RH-CLC reflector reflects only right-circular polarization electroluminescence (RCP-EL) within PBG,. The RCP-EL changes into left-circular polarization electroluminescence (LCP-EL) after refecting the metal electrode. As a result, most LCP-EL light will escape from RH-CLC. Because of special fabrication of CLC film with gradual change of pitch in CLC medium (Figure 3.15 (b)), wide range of PBG was observed from transmittance, covering visible range, as shown in Figure 3.16.

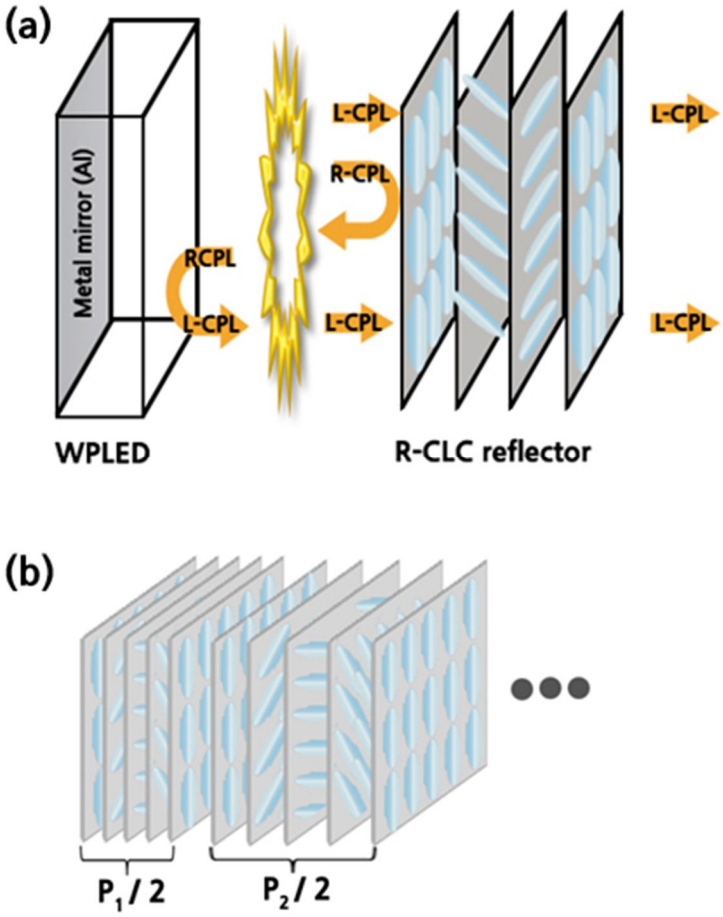

Figure 3.15 (a) The schematic device configuration for highly CP-EL from OLED and (b) corresponding structure of R-CLC reflector.

The intensities of EL with different polarizations were measured and LCP-EL was dominant in WPLEDs combined with RH-CLC reflectors shown in Figure 3.16. In contrast, the intensity of right-circular polarization electroluminescence (RCP-EL) was low within PBG because the RCP-EL is reflected at surface of the R-CLC reflector and changed to L-CLC after reflecting metal electrode of WPLED. As a result, LCP-EL emission occurs dominantly in WPLEDs combined with RH-CLC reflector. Moreover, we measured the performance of WPLEDs to characterize device performance. The *L-V* characteristics of CP-EL of WPLED combined with RH-CLC are shown in Figure 3.17. Either R or L sheet polarizer was used to detect one kind of CP-EL emission. At same operation voltage, the large difference of luminance between LCP-EL and RCP-EL.

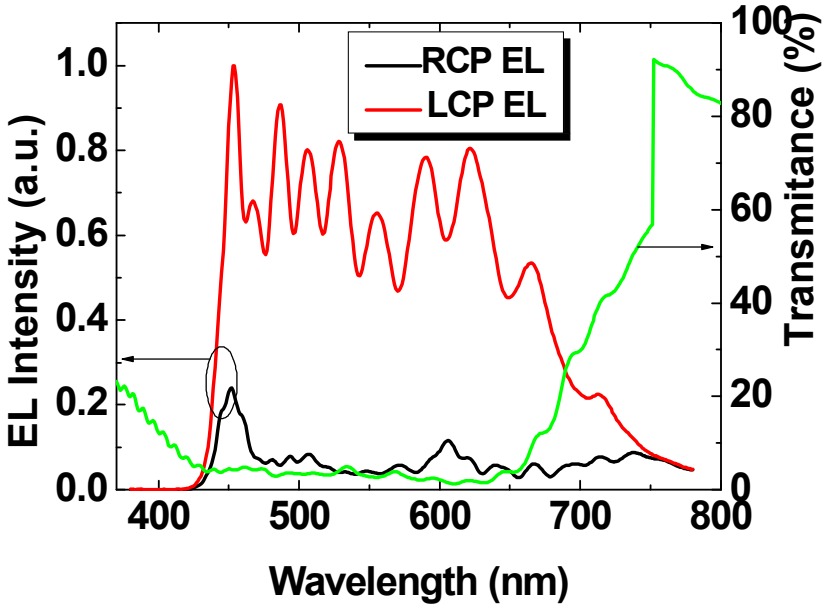

Figure 3.16 R- and L-CP-EL spectra from OLED devices with wide-PCLC films and transmittance spectra of wide-gap R-CLC reflective film.

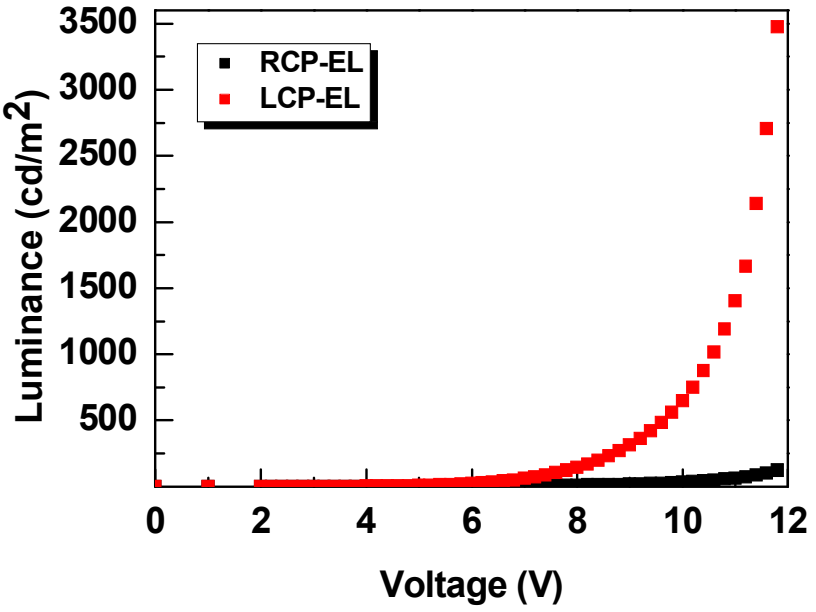

Figure 3.17 Voltage-CP-EL plot of OLEDs with and without PCLC films. R and L polarizers were inserted to measure the R-CP-EL and L-CP-EL.

IV Conclusions

Organic light-emitting diodes (OLEDs) have attracted a great deal of attention, both academic and practical applications for full-color, flat-panel displays and lighting. In particular, polymer light-emitting diodes (PLEDs) have advantages of low-cost processing such as spin coating, dip coating and ink-jet printing in which luminescent polymer solutions are jetted into well defined areas on the substrate. Their future applications of PLEDs include flexible displays which can be folded, wearable displays with interactive feature.

An introduction of semiconducting polymers, device structure and operation of OLEDs and hybrid PLEDs with diverse transition metal oxide (TMO) layer is mainly described in the chapter 1. It is important to outline electronic property of the conjugated polymer adapted in PLEDs. The conductivity of the conjugated polymer is induced by electrons, which are trapped between the carbons, the π-bond electrons have relative mobility. In optical property, the energy difference between valence band and conduction band determines the wavelength (color) of the emitting light.

Based on the basic understanding for the semiconducting properties of the conjugated polymer, the operation of PLEDs using this material can be described as follows. The structure of PLED comprises of a thin film of semiconducting polymer sandwiched between two electrodes (cathode and anode). The operation of OLED/PLED involve charge injection from the electrodes, transport of charge carriers, recombination of holes and electrons to generate electronically excited states, followed by the emission of either fluorescence of phosphorescence.

A recent promising approach to improve the device performances is to use inorganic metal oxide layer such as TiO_2, ZnO, HfO_2, and ZrO_2 as electron injection layer (EIL) and MoO_3 as the hole injection layer (HIL). Hybrid organic-inorganic polymer light-emitting diodes (HyPLEDs) with inorganic metal oxide layer have air-stable property without a low work function metal electrode and compatibility with n-type thin film transistors (TFTs) in backplane for active matrix OLED (AMOLED) applications. Based on this device configuration, interfacial engineering employing hybrid charge transport layer such as n-type metal oxide/self-assembled bipolar molecules (SADMs) is investigated in chapter 1.5.3. The HyPLEDs modified with a negative dipolar SADM exhibited remarkably improved electroluminescence efficiency (2.8 cd/A at 9.6V) and luminance (38000 cd/m^2 at 9.8eV), which is approximately a 4-fold increase compared to those of unmodified HyPLEDs.

Next, a luminescent polymer blend mixed with ionic liquid molecules (ILMs) as active layer in HyPLED configuration is investigated. It is called light-emitting electrochemical cells (LECs) due to unique operation mechanism due to mobile ions in active layer. We demonstrated a straightforward way to enhance the device performance by using a blended film of fluorescent SY polymer and mobile ILMs in hybrid organic-inorganic polymer light-emitting electrochemical cells (HyPLECs)

using ZnO layer. After the redistribution of cations and anions ateach electrode/active layer boundary, the charge injection barriers between each electrode and the active blend layer were reduced and the charge injection and transfer were remarkably enhanced in the corresponding device performance when using pure SY. The modified HyPLECs using ZnO layer with an ILMs (25%) blended into the SY as an active layer exhibited good device performance with low turn-on voltage of 2.1 V, excellent air stability, improved luminance of 3400 cd/m^2, high efficiency of 1.2 cd/A, which is approximately six-fold higher than the electroluminescence efficiency of LECs without ZnO layer. Furthermore, our HyPLECs with SY:ILMs (25 wt % of ILMs) blend showed electroluminescence under reverse bias. This strategy offers a design scheme for improved carrier injection, low turn-on voltage, and high device performance at low operating voltage in air stable hybrid light-emitting devices.

Finally, a red, green and blue (RGB) ternary blend for white emission device was investigated. The blending method has advantages of simpler structure. However, it results in the color shifting with various driving voltages and low efficiency compared to monochromatic OLEDs. The color-shifting phenomenon results from recombination zone shifting, contributing to field-dependent carrier mobilities. We observed stable and highly efficient white PLEDs based on a homogeneous blend of ternary polymers. By diluting the concentration of dopants, a perfect energy transfer between host and dopants is prohibited in polymer blend thus, the device can obtain white-light emission. The device with composition of M-blue : SY : M-red = 99.4 : 0.0075 : 0.5 blend ratio by weight exhibits white emission. The device have EL spectra covering the whole visible range from 400 to 750 nm and exhibited three balanced emission peaks located at the RGB three primary colors. At a concentration of 0.5wt% of M-red doped into M-red host, the CIE coordinates are (0.33, 0.36) corresponding to whitish emission. . The CIE coordinates of the luminescence changed from (x=0.349, y=0.3597) at 7.0V to (x=0.3081, y=0.3335) at 13.6V. The turn-on voltage of the device was 2.4V. The maximum luminance was 10000cd/m^2 at 13.6V. The maximum luminescence efficiency of the polymer LEDs with white polymer blend was 4.67cd/A at 10.8V. By attaching a R-CLC reflector to an WPLED device, we can observe white emission CP-EL. the luminescent difference between LCP-EL and RCP-EL show value of maximum ~1000cd/m^2.

White PLEDs using blue and orange emitting polymer blend in hybrid structure with ZnO layer have been proven to be able to realize the white emission. By mixing M-blue as a host and DCM as orange emitter dye, we can obtain the white light in a single layer. We have successfully obtained pure white emission of (0.3234, 0.3209), corresponding to near the white emission of (0.33, 0.33)

References

[1] Burroughes, J. H., Bradley, D. D. C., Brown, A. R., Marks, R. N., Mackay, K., Friend, R. H., Burns, P. L. & Holmes, A. B. 1990, 'Light-emitting diodes based on conjugated polymers', *Nature*, vol. 347, no. 6293, pp. 539-41.

[2] Mette, H. & Pick, H. 1953, 'Elektronenleitfähigkeit von Anthracen-Einkristallen', *Zeitschrift für Physik A Hadrons and Nuclei*, vol. 134, no. 5, pp. 566-75.

[3] Kepler, R. G. 1960, 'Charge Carrier Production and Mobility in Anthracene Crystals', *Physical Review*, vol. 119, no. 4, pp. 1226-9.

[4] LeBlanc, Jr Oliver H. 1960, 'Hole and Electron Drift Mobilities in Anthracene', *The Journal of Chemical Physics*, vol. 33, no. 2, pp. 626-.

[5] Pope, M., Kallmann, H. P. & Magnante, P. 1963, 'Electroluminescence in Organic Crystals', *The Journal of Chemical Physics*, vol. 38, no. 8, pp. 2042-3.

[6] Chiang, C. K., Fincher, C. R., Jr., Park, Y. W., Heeger, A. J., Shirakawa, H., Louis, E. J., Gau, S. C. & MacDiarmid, Alan G. 1977, 'Electrical Conductivity in Doped Polyacetylene', *Physical Review Letters*, vol. 39, no. 17, pp. 1098-101.

[7] Tang, C. W. & VanSlyke, S. A. 1987, 'Organic electroluminescent diodes', *Applied Physics Letters*, vol. 51, no. 12, pp. 913-5.

[8] Tang, C. W., VanSlyke, S. A. & Chen, C. H. 1989, 'Electroluminescence of doped organic thin films', *Journal of Applied Physics*, vol. 65, no. 9, pp. 3610-6.

[9] Adachi, Chihaya, Tokito, Shizuo, Tsutsui, Tetsuo, Saito, Shogo 1988, 'Electroluminescence in Organic Films with Three-Layer Structure', *Japanese Journal of Applied Physics Part 1-Regular Papers Brief Communications & Review Papers*, vol. 27, no. 27, p. L271.

[10] Hamada, Y., Adachi, C., Tsutsui, T. and Saito, S. 1992, 'Blue-Light-Emitting Organic Electroluminescent Devices with Oxadiazole Dimer Dyes as an Emitter', *Jpn. J. Appl. Phys.*, vol. 31, no. Part 1, No. 6A, pp. 1812-6.

[11] Kido, J., Nagai, K., and Ohashi, Y. 1990, *Chem. Lett.*, vol. 657.

[12] Kido, Junji, Nagai, Katsutoshi & Okamoto, Yoshiyuki 1993, 'Organic electroluminescent devices using lanthanide complexes', *Journal of Alloys and Compounds*, vol. 192, no. 1-2, pp. 30-3.

[13] Kido, Junji, Kohda, Masafumi, Okuyama, Katsuro & Nagai, Katsutoshi 1992, 'Organic electroluminescent devices based on molecularly doped polymers', *Applied Physics Letters*, vol. 61, no. 7, pp. 761-3.

[14] Kido, Junji, Hayase, Hiromichi, Hongawa, Kenichi, Nagai, Katsutoshi & Okuyama, Katsuro 1994, 'Bright red light-emitting organic electroluminescent devices having a europium complex as an emitter', *Applied Physics Letters*, vol. 65, no. 17, pp. 2124-6.

[15] Ohmori, Y., Uchida, M., Muro, K. and Yoshino, K. 1991, 'Visible-Light Electroluminescent Diodes Utilizing Poly(3-alkylthiophene)', *Jpn. J. Appl. Phys.*, vol. 30, no. Part 2, No. 11B, pp. L1938-L40.

[16] Kido, J., Nagai, K., Okamoto, Y. and Skotheim, T. 1991, *Chem. Lett.*, vol. 1267.

[17] Kido, Junji, Nagai, Katsutoshi, Okamoto, Yoshiyuki & Skotheim, Terje 1991, 'Poly(methylphenylsilane) film as a hole transport layer in electroluminescent devices', *Applied Physics Letters*, vol. 59, no. 21, pp. 2760-2.

[18] Kido, J., Kohda, M., Hongawa, K., Okuyama K. and Nagai, K. 1993, 'Molecularly doped polymers for organic electroluminescent devices', *Mol. Cryst. Liq. Cryst.*, vol. 227, pp. pp. 277-83

[19] Kido, J., Guo, Y., McBreen, J. Nagai K. and Okamoto Y. 1992, *Polym. Adv. Tech.*, vol. 3, p. 429.

[20] Kido, Junji, Hongawa, Kenichi, Okuyama, Katsuro & Nagai, Katsutoshi 1993, 'Bright blue electroluminescence from poly(N-vinylcarbazole)', *Applied Physics Letters*, vol. 63, no. 19, pp. 2627-9.

[21] Nalwa, H.S. & Rohwer, L.S. 2003, *Handbook of Luminescence, Display Materials, and Devices: Inorganic display materials*, American Scientific Publishers.

[22] Barford, W. 2005, *Electronic and optical properties of conjugated polymers*, Clarendon Press.

[23] Kittel, C. 1971, *Introduction to solid state physics*, Wiley.

[24] Su, W. P., Schrieffer, J. R. & Heeger, A. J. 1979, 'Solitons in Polyacetylene', *Physical Review Letters*, vol. 42, no. 25, pp. 1698-701.

[25] Waas, V., Büttner, H. & Voit, J. 1990, 'Finite-size studies of phases and dimerization in one-dimensional extended Peierls-Hubbard models', *Physical Review B*, vol. 41, no. 13, pp. 9366-76.

[26] Góra, D and Rosciszewski, K. 1996, 'Spectral density functions for polyacetylene within the Peierls - Hubbard model ', *J. Phys.: Condens. Matter*, vol. 8, p. 8995.

[27] Heeger, A.J., Sariciftci, N.S. & Namdas, E.B. 2010, *Semiconducting and metallic polymers*, Oxford University Press.

[28] Li, Minghang 2010, *Device Engineering for Enhanced Efficiency from Platinum(II) Phosphorescent OLEDs.* , UNT Digital Library, <http://digital.library.unt.edu/ark:/67531/metadc30482/>.

[29] Graupner, Wilhelm, Heller, Christian M., Ghosh, Amalkumar P. & Howard, Webster E. 2000, 'High-resolution color organic light-emitting diode microdisplay fabrication method', SPIE, pp. 11-9.

[30] Chu, Ta-Ya, Chen, Jenn-Fang, Chen, Szu-Yi, Chen, Chao-Jung & Chen, Chin H. 2006, 'Highly efficient and stable inverted bottom-emission organic light emitting devices', *Applied Physics Letters*, vol. 89, no. 5, pp. 053503-3.

[31] Morii, Katsuyuki, Ishida, Masaya, Takashima, Takeshi, Shimoda, Tatsuya, Wang, Qing, Nazeeruddin, Md Khaja & Gratzel, Michael 2006, 'Encapsulation-free hybrid organic-inorganic light-emitting diodes', *Applied Physics Letters*, vol. 89, no. 18, pp. 183510-3.

[32] Haque, S. A, Koops, S., Tokmoldin, N., Durrant, J. R, Huang, J., Bradley, D. D C & Palomares, E. 2007, 'A Multilayered Polymer Light-Emitting Diode Using a Nanocrystalline Metal-Oxide Film as a Charge-Injection Electrode', *Advanced Materials*, vol. 19, no. 5, pp. 683-7.

[33] Kabra, Dinesh, Song, Myoung Hoon, Wenger, Bernard, Friend, Richard H. & Snaith, Henry J. 2008, 'High Efficiency Composite Metal Oxide-Polymer Electroluminescent Devices: A Morphological and Material Based Investigation', *Advanced Materials*, vol. 20, no. 18, pp. 3447-52.

[34] Tokmoldin, Nurlan, Griffiths, Nicholas, Bradley, Donal D. C. & Haque, Saif A. 2009, 'A Hybrid Inorganic–Organic Semiconductor Light-Emitting Diode Using ZrO2 as an Electron-Injection Layer', *Advanced Materials*, vol. 21, no. 34, pp. 3475-8.

[35] Bolink, H. J, Coronado, E., Repetto, D., Sessolo, M., Barea, E. M, Bisquert, J., Garcia-Belmonte, G., Prochazka, J. & Kavan, L. 2008, 'Inverted Solution Processable OLEDs Using a Metal Oxide as an Electron Injection Contact', *Advanced Functional Materials*, vol. 18, no. 1, pp. 145-50.

[36] Morii, Katsuyuki, Kawase, Takeo & Inoue, Satoshi 2008, 'High efficiency and stability in air of the encapsulation-free hybrid organic-inorganic light-emitting diode', *Applied Physics Letters*, vol. 92, no. 21, pp. 213304-3.

[37] Bolink, Henk J., Coronado, Eugenio, Orozco, Javier & Sessolo, Michele 2009, 'Efficient Polymer Light-Emitting Diode Using Air-Stable Metal Oxides as Electrodes', *Advanced Materials*, vol. 21, no. 1, pp. 79-82.

[38] Chen, Xiaobo & Mao, Samuel S. 2007, 'Titanium Dioxide Nanomaterials: Synthesis, Properties, Modifications, and Applications', *Chemical Reviews*, vol. 107, no. 7, pp. 2891-959.

[39] Ozgur, U., Alivov, Ya I., Liu, C., Teke, A., Reshchikov, M. A., Dogan, S., Avrutin, V., Cho, S. J. & Morkoc, H. 2005, 'A comprehensive review of ZnO materials and devices', *Journal of Applied Physics*, vol. 98, no. 4, pp. 041301-103.

[40] Morii, K., Omoto, M., Ishida, M. and Graetzel, M. 2008, 'Enhanced Hole Injection in a Hybrid Organic–Inorganic Light-Emitting Diode', *Jpn. J. Appl. Phys.*, vol. 47, no. 9, pp. pp.7366-8.

[41] Park, Ji Sun, Lee, Bo Ram, Lee, Ju Min, Kim, Ji-Seon, Kim, Sang Ouk & Song, Myoung Hoon 2010, 'Efficient hybrid organic-inorganic light emitting diodes with self-assembled dipole molecule deposited metal oxides', *Applied Physics Letters*, vol. 96, no. 24, pp. 243306-3.

[42] Park, Ji Sun, Lee, Bo Ram, Jeong, Eunjae, Lee, Hyun-Jung, Lee, Ju Min, Kim, Ji-Seon, Kim, Jin Young, Woo, Han Young, Kim, Sang Ouk & Song, Myoung Hoon 2011, 'High performance polymer light-emitting diodes with N-type metal oxide/conjugated polyelectrolyte hybrid charge transport layers', *Applied Physics Letters*, vol. 99, no. 16, pp. 163305-3.

[43] Bolink, Henk J., Coronado, Eugenio, Repetto, Diego & Sessolo, Michele 2007, 'Air stable hybrid organic-inorganic light emitting diodes using ZnO as the cathode', *Applied Physics Letters*, vol. 91, no. 22, pp. 223501-3.

[44] Kabra, Dinesh, Lu, Li Ping, Song, Myoung Hoon, Snaith, Henry J. & Friend, Richard H. 2010, 'Efficient Single-Layer Polymer Light-Emitting Diodes', *Advanced Materials*, vol. 22, no. 29, pp. 3194-8.

[45] Lee, Tae-Woo, Hwang, Joohyun & Min, Sung-Yong 2010, 'Highly Efficient Hybrid Inorganic–Organic Light-Emitting Diodes by using Air-Stable Metal Oxides and a Thick Emitting Layer', *ChemSusChem*, vol. 3, no. 9, pp. 1021-3.

[46] Nakayama, Yasuo, Morii, Katsuyuki, Suzuki, Yuuichirou, Machida, Hiroyuki, Kera, Satoshi, Ueno, Nobuo, Kitagawa, Hiroshi, Noguchi, Yutaka & Ishii, Hisao 2009, 'Origins of Improved Hole-Injection Efficiency by the Deposition of MoO3 on the Polymeric Semiconductor Poly(dioctylfluorene-alt-benzothiadiazole)', *Advanced Functional Materials*, vol. 19, no. 23, pp. 3746-52.

[47] Chu, Chih-Wei, Li, Sheng-Han, Chen, Chieh-Wei, Shrotriya, Vishal & Yang, Yang 2005, 'High-performance organic thin-film transistors with metal oxide/metal bilayer electrode', *Applied Physics Letters*, vol. 87, no. 19, pp. 193508-3.

[48] You, Han, Dai, Yanfeng, Zhang, Zhiqiang & Ma, Dongge 2007, 'Improved performances of organic light-emitting diodes with metal oxide as anode buffer', *Journal of Applied Physics*, vol. 101, no. 2, pp. 026105-3.

[49] Brabec, Christoph J., Shaheen, Sean E., Winder, Christoph, Sariciftci, N. Serdar & Denk, Patrick 2002, 'Effect of LiF/metal electrodes on the performance of plastic solar cells', *Applied Physics Letters*, vol. 80, no. 7, pp. 1288-90.

[50] Hoven, Corey V., Yang, Renqiang, Garcia, Andres, Crockett, Victoria, Heeger, Alan J., Bazan, Guillermo C. & Nguyen, Thuc-Quyen 2008, 'Electron injection into organic semiconductor devices from high work function cathodes', *Proceedings of the National Academy of Sciences*, vol. 105, no. 35, pp. 12730-5.

[51] Lee, Bo Ram, Choi, Hyosung, SunPark, Ji, Lee, Hyun Jung, Kim, Sang Ouk, Kim, Jin Young & Song, Myoung Hoon 2011, 'Surface modification of metal oxide using ionic liquid molecules in hybrid organic-inorganic optoelectronic devices', *Journal of Materials Chemistry*, vol. 21, no. 7, pp. 2051-3.

[52] Yip, Hin-Lap, Hau, Steven K., Baek, Nam Seob, Ma, Hong & Jen, Alex K. Y. 2008, 'Polymer Solar Cells That Use Self-Assembled-Monolayer- Modified ZnO/Metals as Cathodes', *Advanced Materials*, vol. 20, no. 12, pp. 2376-82.

[53] Pei, Qibing, Yu, Gang, Zhang, Chi, Yang, Yang & Heeger, Alan J. 1995, 'Polymer Light-Emitting Electrochemical Cells', *Science*, vol. 269, no. 5227, pp. 1086-8.

[54] Pei, Qibing, Yang, Yu, Gang, Zhang, Chi & Heeger, Alan J. 1996, 'Polymer Light-Emitting Electrochemical Cells: In Situ Formation of a Light-Emitting p−n Junction', *Journal of the American Chemical Society*, vol. 118, no. 16, pp. 3922-9.

[55] Yang, Chunhe, Sun, Qingjiang, Qiao, Jing & Li, Yongfang 2003, 'Ionic Liquid Doped Polymer Light-Emitting Electrochemical Cells', *The Journal of Physical Chemistry B*, vol. 107, no. 47, pp. 12981-8.

[56] Marcilla, Rebeca, Mecerreyes, David, Winroth, Gustaf, Brovelli, Sergio, Yebra, Maria del Mar Rodriguez & Cacialli, Franco 2010, 'Light-emitting electrochemical cells using polymeric ionic liquid/polyfluorene blends as luminescent material', *Applied Physics Letters*, vol. 96, no. 4, pp. 043308-3.

[57] Shao, Y., Bazan, G. C & Heeger, A. J 2007, 'Long-Lifetime Polymer Light-Emitting Electrochemical Cells', *Advanced Materials*, vol. 19, no. 3, pp. 365-70.

[58] Jin, Youngeup, Bazan, Guillermo C., Heeger, Alan J., Kim, Jin Young & Lee, Kwanghee 2008, 'Improved electron injection in polymer light-emitting diodes using anionic conjugated

polyelectrolyte', *Applied Physics Letters*, vol. 93, no. 12, pp. 123304-3.

[59] deMello, John C. 2007, 'Organic electronics: What's in a name?', *Nat Mater*, vol. 6, no. 11, pp. 796-7.

[60] Hatwar, Tukaram K. 2004, 'High-efficiency white OLEDs based on small molecules', vol. 5214, pp. 233-40.

[61] Liedtke, Alicia, O'Neill, Mary, Wertmöller, Anke, Kitney, Stuart P. & Kelly, Stephen M. 2008, 'White-Light OLEDs Using Liquid Crystal Polymer Networks', *Chemistry of Materials*, vol. 20, no. 11, pp. 3579-86.

[62] Kido, J., Kimura, M. & Nagai, K. 1995, 'Multilayer White Light-Emitting Organic Electroluminescent Device', *Science*, vol. 267, no. 5202, pp. 1332-4.

[63] Jordan, R. H., Dodabalapur, A., Strukelj, M. & Miller, T. M. 1996, 'White organic electroluminescence devices', *Applied Physics Letters*, vol. 68, no. 9, pp. 1192-4.

[64] Wang, Y. Z., Sun, R. G., Meghdadi, F., Leising, G. & Epstein, A. J. 1999, 'Multicolor multilayer light-emitting devices based on pyridine-containing conjugated polymers and para-sexiphenyl oligomer', *Applied Physics Letters*, vol. 74, no. 24, pp. 3613-5.

[65] Kido, J., Shionoya, H. & Nagai, K. 1995, 'Single-layer white light-emitting organic electroluminescent devices based on dye-dispersed poly(N-vinylcarbazole)', *Applied Physics Letters*, vol. 67, no. 16, pp. 2281-3.

[66] Hwang, D. H., Park, M. J., Kim, S. K., Lee, N. H., Lee, C., Kim, Y. B. & Shim, H. K. 2004, 'Characterization of white electroluminescent devices fabricated using conjugated polymer blends', *Journal of Materials Research*, vol. 19, no. 7, pp. 2081-6.

[67] Kido, J., Hongawa, K., Okuyama, K. & Nagai, K. 1994, 'White light-emitting organic electroluminescent devices using the poly(N-vinylcarbazole) emitter layer doped with three fluorescent dyes', *Applied Physics Letters*, vol. 64, no. 7, pp. 815-7.

[68] Hu, B. & Karasz, F. E. 2003, 'Blue, green, red, and white electroluminescence from

multichromophore polymer blends', *Journal of Applied Physics*, vol. 93, no. 4, pp. 1995-2001.

[69] Higgins, R. W. T., Monkman, A. P., Nothofer, H. G. & Scherf, U. 2001, 'Effects of singlet and triplet energy transfer to molecular dopants in polymer light-emitting diodes and their usefulness in chromaticity tuning', *Applied Physics Letters*, vol. 79, no. 6, pp. 857-9.

[70] Chang, S. M., Tzeng, Y. J., Wu, S. Y., Li, K. Y. & Hsueh, K. L. 2005, 'Emission of white light from 2-(2 '-hydroxyphenyl) benzothiazole in polymer electroluminescent devices', *Thin Solid Films*, vol. 477, no. 1-2, pp. 38-41.

[71] Kim, J. H., Herguth, P., Kang, M. S., Jen, A. K. Y., Tseng, Y. H. & Shu, C. F. 2004, 'Bright white light electroluminescent devices based on a dye-dispersed polyfluorene derivative', *Applied Physics Letters*, vol. 85, no. 7, pp. 1116-8.

[72] Kim, S., Seo, J., Jung, H. K, Kim, J. J. & Park, S. Y 2005, 'White Luminescence from Polymer Thin Films Containing Excited-State Intramolecular Proton-Transfer Dyes', *Advanced Materials*, vol. 17, no. 17, pp. 2077-82.

[73] Mikami, A., Koshiyama, T. & Tsubokawa, T. 2005, 'High-efficiency color and white organic light-emitting devices prepared on flexible plastic substrates', *Japanese Journal of Applied Physics Part 1-Regular Papers Brief Communications & Review Papers*, vol. 44, no. 1B, pp. 608-12.

[74] Gong, X., Wang, S., Moses, D., Bazan, G. C & Heeger, A. J 2005, 'Multilayer Polymer Light-Emitting Diodes: White-Light Emission with High Efficiency', *Advanced Materials*, vol. 17, no. 17, pp. 2053-8.

[75] Tanaka, I., Suzuki, M. & Tokito, S. 2003, 'White light emission from polymer electrophosphorescent light-emitting devices doped with iridium complexes', *Japanese Journal of Applied Physics Part 1-Regular Papers Short Notes & Review Papers*, vol. 42, no. 5A, pp. 2737-40.

[76] Hino, Y., Kajii, H. & Ohmori, Y. 2006, 'Transient characteristics of polyfluorene-based polymer light-emitting diodes and their application for color tunable devices', *Thin Solid Films*, vol. 499, no. 1-2, pp. 359-63.

[77] Liu, J., Zhou, Q. G, Cheng, Y. X, Geng, Y. H, Wang, L. X, Ma, D. G, Jing, X. B & Wang,

F. S 2005, 'The First Single Polymer with Simultaneous Blue, Green, and Red Emission for White Electroluminescence', *Advanced Materials*, vol. 17, no. 24, pp. 2974-8.

[78] Tu, G. L, Mei, C. Y, Zhou, Q. G, Cheng, Y. X, Geng, Y. H, Wang, L. X, Ma, D. G, Jing, X. B & Wang, F. S 2006, 'Highly Efficient Pure-White-Light-Emitting Diodes from a Single Polymer: Polyfluorene with Naphthalimide Moieties', *Advanced Functional Materials*, vol. 16, no. 1, pp. 101-6.

[79] Geoghegan, Mark, Ermer, Hubert, Jüngst, Gerald, Krausch, Georg & Brenn, Rüdiger 2000, 'Wetting in a phase separating polymer blend film: Quench depth dependence', *Physical Review E*, vol. 62, no. 1, pp. 940-50.

[80] Popescu, Lacramioara M., van 't Hof, Patrick, Sieval, Alexander B., Jonkman, Harry T. & Hummelen, Jan C. 2006, 'Thienyl analog of 1-(3-methoxycarbonyl)propyl-1-phenyl-[6,6]-methanofullerene for bulk heterojunction photovoltaic devices in combination with polythiophenes', *Applied Physics Letters*, vol. 89, no. 21, pp. 213507-3.

[81] Kuhlmann, Jan-Carlos, Bruyn, Paul de, Bouwer, Ricardo K. M., Meetsma, Auke, Blom, Paul W. M. & Hummelen, Jan C. 2010, 'Improving the compatibility of fullerene acceptors with fluorene-containing donor-polymers in organic photovoltaic devices', *Chemical Communications*, vol. 46, no. 38, pp. 7232-4.

[82] Yang, J. P., Jin, Y. D., Heremans, P. L., Hoefnagels, R., Dieltiens, P., Blockhuys, F., Geise, H. J., Van der Auweraer, M. & Borghs, G. 2000, 'White light emission from a single layer organic light emitting diode fabricated by spincoating', *Chemical Physics Letters*, vol. 325, no. 1-3, pp. 251-6.

[83] Van Der Meer, B. W., Coker III, G. Simon Chen, S.-Y. 1994, *Resonance Energy Transfer, Theory and Data*, VCH, Weinheim, Germany.

[84] Förster, T. 1959, *Discuss. Faraday Soc.*, vol. 27, p. 7.

[85] Jae-Woong Yua, Jai Kyeong Kim, Dong Young Kim, Chul hee Kim, Nam Woong Song. Dongho Kim 2006, 'Prediction of efficient energy transfer in emissive polymer blends based on Förster radius and the excited state lifetime of acceptors', *Current Applied Physics*, vol. 6, no. 1, pp. 59-65.

[86] Gupta, R., Stevenson, M., Dogariu, A., McGehee, M. D., Park, J. Y., Srdanov, V., Heeger, A. J. & Wang, H. 1998, 'Low-threshold amplified spontaneous emission in blends of conjugated polymers', *Applied Physics Letters*, vol. 73, no. 24, pp. 3492-4.

[87] Hojin, Lee, Johnson, A. R. & Kanicki, J. 2006, 'White LED based on polyfluorene Co-polymers blend on plastic substrate', *Electron Devices, IEEE Transactions on*, vol. 53, no. 3, pp. 427-34.

[88] De Gennes, P.G., Prost, J. 1993, *The physics of liquid crystals, 2nd ed.*, Clarendon Press, Oxford.

[89] Chandrasekhar, S. 1992, *Liquid Crystals*, Cambridge University Press, Cambridge.

[90] Meskers, S. C. J., Peeters, E., Langeveld-Voss, B. M. W. & Janssen, R. A. J. 2000, 'Circular Polarization of the Fluorescence from Films of Poly(p-phenylene vinylene) and Polythiophene with Chiral Side Chains', *Advanced Materials*, vol. 12, no. 8, pp. 589-94.

[91] Pollmann, P., Mainusch, K. J. & Stegemeyer, H. 1976, 'CIRCULAR-POLARIZATION OF FLUORESCENCE OF ACHIRAL MOLECULES IN CHOLESTERIC LIQUID-CRYSTALS', *Zeitschrift Fur Physikalische Chemie-Frankfurt*, vol. 103, no. 5-6, pp. 295-309.

[92] Chen, S. H., Katsis, D., Schmid, A. W., Mastrangelo, J. C., Tsutsui, T. & Blanton, T. N. 1999, 'Circularly polarized light generated by photoexcitation of luminophores in glassy liquid-crystal films', *Nature*, vol. 397, no. 6719, pp. 506-8.

[93] Langeveld-Voss, B. M. W., Janssen, R. A. J., Christiaans, M. P. T., Meskers, S. C. J., Dekkers, H. P. J. M. & Meijer, E. W. 1996, 'Circular Dichroism and Circular Polarization of Photoluminescence of Highly Ordered Poly{3,4-di[(S)-2-methylbutoxy]thiophene}', *Journal of the American Chemical Society*, vol. 118, no. 20, pp. 4908-9.

[94] Peeters, E., Christiaans, M. P. T., Janssen, R. A. J., Schoo, H. F. M., Dekkers, Hpjm & Meijer, E. W. 1997, 'Circularly polarized electroluminescence from a polymer light-emitting diode', *Journal of the American Chemical Society*, vol. 119, no. 41, pp. 9909-10.

[95] Belayev, S. V., Schadt, M., Barnik, M. I., Funfschilling, J., Malimoneko, N. V. & Schmitt, K. 1990, 'LARGE APERTURE POLARIZED-LIGHT SOURCE AND NOVEL LIQUID-CRYSTAL DISPLAY OPERATING MODES', *Japanese Journal of Applied Physics Part 2-Letters*, vol. 29, no. 4,

pp. L634-L7.

Acknowledgement

I owe the deepest gratitude to my supervisor, Prof. Myoung Hoon Song. His encouragement, inspiration, guidance and support enabled me to develop an understanding of the research. I feel very lucky to be under the direction of Prof. Myoung Hoon Song at UNIST.

I want to express my gratitude to Prof. Jin Young Kim, Prof. Jeong Min Baik for giving me advice about my research as a committee and Prof. Soon-Yong Kwon for cheering me up with sincere words.

Thanks to Ph.D. Ji Sun Park (at KAIST) for giving me so much help, teaching me everything in the laboratory. I followed her and I could obtain not only experimental techniques but also personal assistances.

I would like to thank my lab members, NGEL members, Nuclear research group (UNIST) and office members. They gave me a valuable advice and encouragement. Above all, I would like to show my gratitude to many friends who I met at UNIST. I am grateful to Sarah Kang, Eunju Park, Jiwoon Park and Heungseok Go (PaxGO). Their warm affection encouraged me a lot so I could withstand lonely and hard time in Ulsan. Finally, I acknowledge many people who help me every time I asked them.

Curriculum Vitae

Hyun Jung Lee

M.S.

School of Mechanical and Advanced Materials Engineering

Ulsan National Institute of Science and Technology (UNIST), Ulsan City, Republic of Korea

Mobile : +82-10-4018-1291

E-mail : hj1291@unist.ac.kr

EDUCATION

M.S, Advanced Materials Engineering, 2012, UNIST, Ulsan, Republic of Korea

B.A, Chemical Engineering, 2010, Chonbuk National University, Jeonju, Republic of Korea

RESEARCH INTERESTS

- Polymer light-emitting diodes (PLEDs)
- Polymer light-emitting electrochemical cells (PLECs)
- Optoelectronic devices

RESEARCH PUBRICATIONS

1. Park, Ji Sun, Lee, Bo Ram, Jeong, Eunjae, **Lee, Hyun-Jung**, Lee, Ju Min, Kim, Ji-Seon, Kim, Jin Young, Woo, Han Young, Kim, Sang Ouk & Song, Myoung Hoon 2011, 'High performance polymer light-emitting diodes with N-type metal oxide/conjugated polyelectrolyte hybrid charge transport layers', *Applied Physics Letters*, vol. 99, no. 16, pp. 163305-3.

2. **Lee, Hyun Jung**, Lee, Bo Ram, Park, Ji Sun, Kim, Sang Ouk, Kim, Jin Young & Song, Myoung Hoon 2011, 'Hybrid organic-inorganic light-emitting electrochemical cells using fluorescent polymer and ionic liquid blend as an active layer', *Applied Physics Letters*, vol. 98, no. 25, pp. 253309-3.

3. Lee, Bo Ram, Choi, Hyosung, Park, Ji Sun, **Lee, Hyun Jung**, Kim, Sang Ouk, Kim, Jin Young & Song, Myoung Hoon 2011, 'Surface modification of metal oxide using ionic liquid molecules in hybrid organic-inorganic optoelectronic devices', *Journal of Materials Chemistry*, vol. 21, no. 7, pp. 2051-3.

CONFERENCES

1. **Hyun Jung Lee**, Jin Young Kim, Myoung Hoon Song, "Hybrid inorganic-organic light-emitting electrochemical cells using fluorescent polymer/ionic liquid blends as active medium", **The Polymer Society of Korea Fall Meeting**, Oct 7-8, 2010, Daegu Exhibition & Convention Center (Exco), Daegu, Republic of Korea